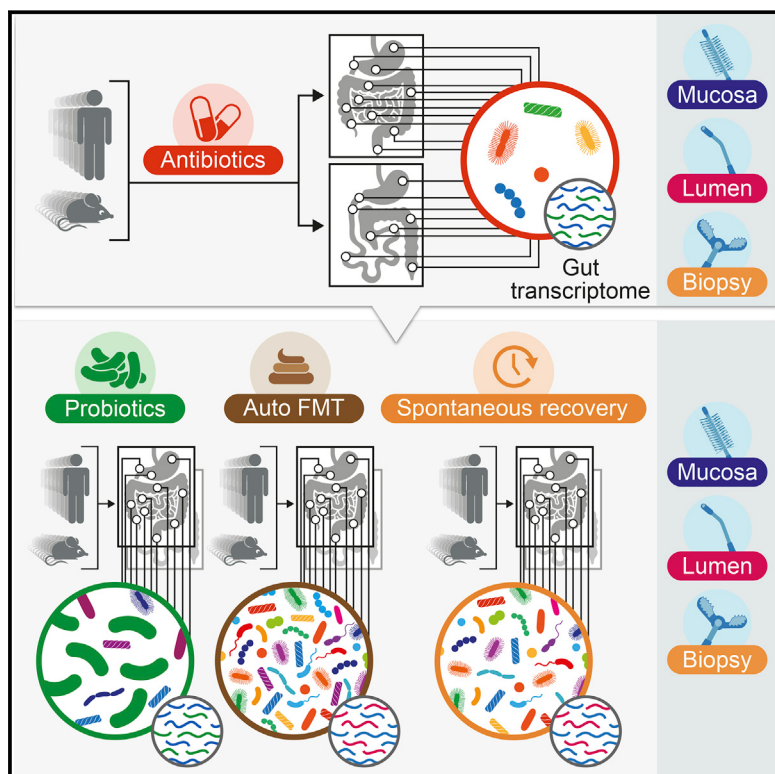


Post-Antibiotic Gut Mucosal Microbiome Reconstitution Is Impaired by Probiotics and Improved by Autologous FMT

Graphical Abstract



Authors

Jotham Suez, Niv Zmora,
Gili Zilberman-Schapira, ...,
Zamir Halpern, Eran Segal, Eran Elinav

Correspondence

zamir@tlvmc.gov.il (Z.H.),
eran.segal@weizmann.ac.il (E.S.),
eran.elinav@weizmann.ac.il (E.E.)

In Brief

Probiotics perturb rather than aid in microbiota recovery back to baseline after antibiotic treatment in humans.

Highlights

- Murine gut mucosal probiotic colonization is only mildly enhanced by antibiotics
- Human gut mucosal probiotic colonization is significantly enhanced by antibiotics
- Post antibiotics, probiotics delay gut microbiome and transcriptome reconstitution
- In contrast, aFMT restores mucosal microbiome and gut transcriptome reconstitution



Post-Antibiotic Gut Mucosal Microbiome Reconstitution Is Impaired by Probiotics and Improved by Autologous FMT

Jotham Suez,^{1,11} Niv Zmora,^{1,2,11} Gili Zilberman-Schapira,^{1,11} Uria Mor,^{1,11} Mally Dori-Bachash,¹ Stavros Bashiardes,¹ Maya Zur,¹ Dana Regev-Lehavi,¹ Rotem Ben-Zeef Brik,¹ Sara Federici,¹ Max Horn,¹ Yotam Cohen,¹ Andreas E. Moor,³ David Zeevi,^{3,4} Tal Korem,^{3,4} Eran Kotler,^{3,4} Alon Harmelin,⁵ Shalev Itzkovitz,³ Nitsan Maharshak,^{6,7,8} Oren Shibolet,^{6,7,8} Meirav Pevsner-Fischer,¹ Hagit Shapiro,¹ Itai Sharon,^{9,10} Zamir Halpern,^{6,7,8,12,*} Eran Segal,^{3,4,12,*} and Eran Elinav^{1,12,13,*}

¹Immunology Department, Weizmann Institute of Science, 7610001 Rehovot, Israel

²Internal Medicine Department, Tel Aviv Sourasky Medical Center, 6423906 Tel Aviv, Israel

³Department of Molecular Cell Biology, Weizmann Institute of Science, 7610001 Rehovot, Israel

⁴Department of Computer Science and Applied Mathematics, Weizmann Institute of Science, 7610001 Rehovot, Israel

⁵Department of Veterinary Resources, Weizmann Institute of Science, 7610001 Rehovot, Israel

⁶Department of Gastroenterology and Liver Diseases, Tel Aviv Sourasky Medical Center, 6423906 Tel Aviv, Israel

⁷Research Center for Digestive tract and Liver Diseases, Tel Aviv Sourasky Medical Center, 6423906 Tel Aviv, Israel

⁸Sackler Faculty of Medicine, Tel Aviv University, 6997801 Tel Aviv, Israel

⁹Migal Galilee Research Institute, 11016 Kiryat Shmona, Israel

¹⁰Tel Hai College, Upper Galilee, 1220800, Israel

¹¹These authors contributed equally

¹²Senior author

¹³Lead Contact

*Correspondence: zamir@tlvmc.gov.il (Z.H.), eran.segal@weizmann.ac.il (E.S.), eran.elinav@weizmann.ac.il (E.E.)
<https://doi.org/10.1016/j.cell.2018.08.047>

SUMMARY

Probiotics are widely prescribed for prevention of antibiotics-associated dysbiosis and related adverse effects. However, probiotic impact on post-antibiotic reconstitution of the gut mucosal host-microbiome niche remains elusive. We invasively examined the effects of multi-strain probiotics or autologous fecal microbiome transplantation (aFMT) on post-antibiotic reconstitution of the murine and human mucosal microbiome niche. Contrary to homeostasis, antibiotic perturbation enhanced probiotics colonization in the human mucosa but only mildly improved colonization in mice. Compared to spontaneous post-antibiotic recovery, probiotics induced a markedly delayed and persistently incomplete indigenous stool/mucosal microbiome reconstitution and host transcriptome recovery toward homeostatic configuration, while aFMT induced a rapid and near-complete recovery within days of administration. *In vitro*, *Lactobacillus*-secreted soluble factors contributed to probiotics-induced microbiome inhibition. Collectively, potential post-antibiotic probiotic benefits may be offset by a compromised gut mucosal recovery, highlighting a need of developing aFMT or personalized probiotic approaches achieving mucosal protection without compromising microbiome recolonization in the antibiotics-perturbed host.

INTRODUCTION

Antibiotics have transformed medicine and the fight against common life-threatening bacterial infections (Van Boekel et al., 2014). However, widespread antibiotic exposure is associated with the emergence of resistant strains and with a variety of gastrointestinal (GI) effects, hypersensitivity, and drug-specific adverse effects, most notably antibiotic-associated diarrhea (AAD) in 5% to 35% of treated humans (Wiström et al., 2001, McFarland, 1998). Non-selective antibiotics-induced disruption of commensal microbiome community structure (“dysbiosis”) accounts for up to 20% of all AAD cases (Bartlett, 2002). Such dysbiosis occurs rapidly within days, leading to altered bacterial metabolism and impaired host proteome in mice and humans (Ferrer et al., 2014, Lichtman et al., 2016). Human microbiome reconstitution from antibiotic treatment is often slow and incomplete (Dethlefsen et al., 2008, Dethlefsen and Relman, 2011, Jernberg et al., 2007) and, in some cases, may take years to revert to naive configuration (Lankelma et al., 2017). Of note, studies in rodent models and humans suggest an association between antibiotic exposure, especially during early stages of life, and a host propensity for a variety of long-term disorders (Vangay et al., 2015), including obesity (Shao et al., 2017), allergy (Risnes et al., 2011, Hoskin-Parr et al., 2013), increased risk of autoimmunity (Arponen et al., 2015), and inflammatory bowel disease (Virta et al., 2012, Kronman et al., 2012).

Probiotics have been proposed to constitute an effective preventive treatment for antibiotics-induced dysbiosis and associated adverse effects in mice (Ekmekciu et al., 2017) and in some (Hempel et al., 2012) but not all human studies (Olek et al., 2017, Allen et al., 2013). Importantly, adverse effects



associated with probiotics consumption may be under-reported in clinical trials (Bafeta et al., 2018), further complicating the efficacy debate. The extent and pattern of probiotic gut mucosal colonization and impact on the indigenous gut microbiome following antibiotic use also remain unclear. While few small-scale culture-based studies attempted to quantify supplemented probiotics in the antibiotics-perturbed GI mucosa (Klarin et al., 2005), the vast majority of studies extrapolate their conclusions from stool samples, resulting in inconclusive findings regarding probiotics capability to restore the pre-antibiotics microbiome configuration (McFarland, 2014). Importantly, no *in vivo* studies have directly examined the global extent of human mucosal probiotic colonization following antibiotic treatment and their impact on reconstitution of the indigenous mucosal microbiome or the host gut transcriptome.

Here, we explored the impact of probiotics consumption following antibiotic exposure on the gut luminal, mucosal, and fecal microbiome composition and function and the GI transcriptome in mice and humans. To this aim, mice and a cohort of human volunteers were treated with broad-spectrum antibiotics and then either were supplemented with probiotics, underwent autologous fecal microbiome transplantation (aFMT), or were allowed to spontaneously recover over time. We found significant differences between mice and humans with respect to post-antibiotic probiotics gut mucosal colonization. Mice featured only a mild improvement in colonization of the “human-compatible” probiotics regimen upon antibiotic treatment as compared to homeostatic conditions, while humans demonstrated a marked colonization improvement in this setting. Importantly, post-antibiotic probiotic supplementation significantly delayed the extent of reconstitution of the indigenous fecal and mucosal microbiome (in both mice and humans) and the reversion of the gut transcriptome toward homeostatic configuration (in humans) compared to either spontaneous reconstitution or aFMT. In contrast, post-antibiotic aFMT in both mice and humans achieved a rapid and near-complete gut mucosal microbiome recolonization associated with reversion of the human gut transcriptome toward its pre-antibiotic configuration.

RESULTS

Experimental Setup in Mice

Under homeostatic conditions (Zmora et al., 2018), administration of a multi-strain probiotic preparation was associated with limited colonization in mice and with person-specific gut mucosal colonization resistance in humans. To study the post-antibiotic mucosal colonization capacity of probiotics and their impact on the indigenous mucosal microbiome as compared to aFMT or watchful waiting, we performed the MUCosal Search for Probiotic Impact and Colonization 3 (MUSPIC3) study in mice and in humans. In mice, we supplemented the drinking water of adult male wild-type (WT) C57BL/6 mice with a broad-spectrum antibiotic regimen of ciprofloxacin and metronidazole for 2 weeks. The immediate impact of antibiotic treatment on gut mucosal microbiome configuration was assessed in one group of mice sacrificed after the 2-week antibiotic exposure (Figure 1A, “Antibiotics”). The remaining animals ($n = 30$) were divided into three post-antibiotic intervention groups. In the first

group (“Probiotics”), antibiotic treatment was followed by 4 weeks of daily administration by oral gavage of a commercially prescribed probiotics product involving 11 strains that was validated for composition and viability by multiple methods (Zmora et al., 2018): *Lactobacillus acidophilus* (LAC), *L. casei* (LCA), *L. casei* ssp. *paracasei* (LPA), *L. plantarum* (LPL), *L. rhamnosus* (LRH), *Bifidobacterium longum* (BLO), *B. bifidum* (BBI), *B. breve* (BBR), *B. longum* ssp. *infantis* (BIN), *Lactococcus lactis* (LLA), and *Streptococcus thermophilus* (STH). Each mouse of the second group (“aFMT”) received, on the day following cessation of antibiotics, an oral gavage of its own pre-antibiotics stool microbiome. A third group (“Spontaneous”) remained untreated following antibiotic therapy to assess the spontaneous recovery of the indigenous gut microbiome in this setting. An additional group of mice (“Control”) did not receive antibiotics or any other treatment and was followed throughout the study’s duration.

Antibiotic Treatment Mildly Enhances Probiotic Gut Mucosal Colonization in Mice

We first assessed the fecal and mucosal colonization of probiotics following broad-spectrum antibiotic treatment in mice. 16S rDNA indicated that three of the four genera comprising the probiotics mix (*Lactobacillus*, *Bifidobacterium*, and *Streptococcus*) were present in stool samples even prior to antibiotic administration (Figures S1A–S1C). 1 day following probiotics administration, *Lactobacillus* (Figure S1A), *Bifidobacterium* (Figure S1B), and *Lactococcus* genera (Figure S1D) increased in relative abundance (RA). On day 4, only *Bifidobacterium* RA remained elevated, after which none of the genera RAs were significantly higher in the treated group (Figures S1A–S1D). Given the inability of 16S rDNA analysis to distinguish absolute abundance changes at the species level, we utilized a sensitive species-specific qPCR (Zmora et al., 2018) targeting each of the tested 11-probiotic species. A pooled qPCR analysis for all species in stool indicated >10,000-fold fecal enrichment of probiotic species on days 1 and 4 of probiotic supplementation (Figure 1B), which rapidly declined in the following days, thereby losing statistical significance, though the trend persisted throughout the experiment (incremental area under the curve [iAUC] $p < 0.0001$ versus each group). A per-species analysis indicated 9 of the 11 species (all but BBI and LAC) to be significantly enriched in stool during probiotics supplementation (Figure 1C).

Like in stool, 16S rDNA assessment of mucosal gut surfaces did not detect a significant elevation in the RA of any of the probiotics genera in any of the regions (Figures S1E–S1H). A pooled qPCR analysis for all administered probiotic species indicated significantly higher abundance in the lumen of the lower GI (LGI), but not the LGI mucosa (Figure 1D) or the upper GI (UGI; Figure 1E). The species that were significantly elevated in the lumen of the LGI tissues and the stomach were consistent with those shed in stool, while only BBR, LRH, and STH were significantly elevated in the LGI mucosa (Figure 1F). In comparison, mice that received probiotics using the same experimental design but without antibiotics pre-treatment featured a significantly lower aggregated probiotics load of all targets in the GI lumen, but not the mucosa (Figure S2A). These results indicate that resistance to the presence of probiotic species in the murine

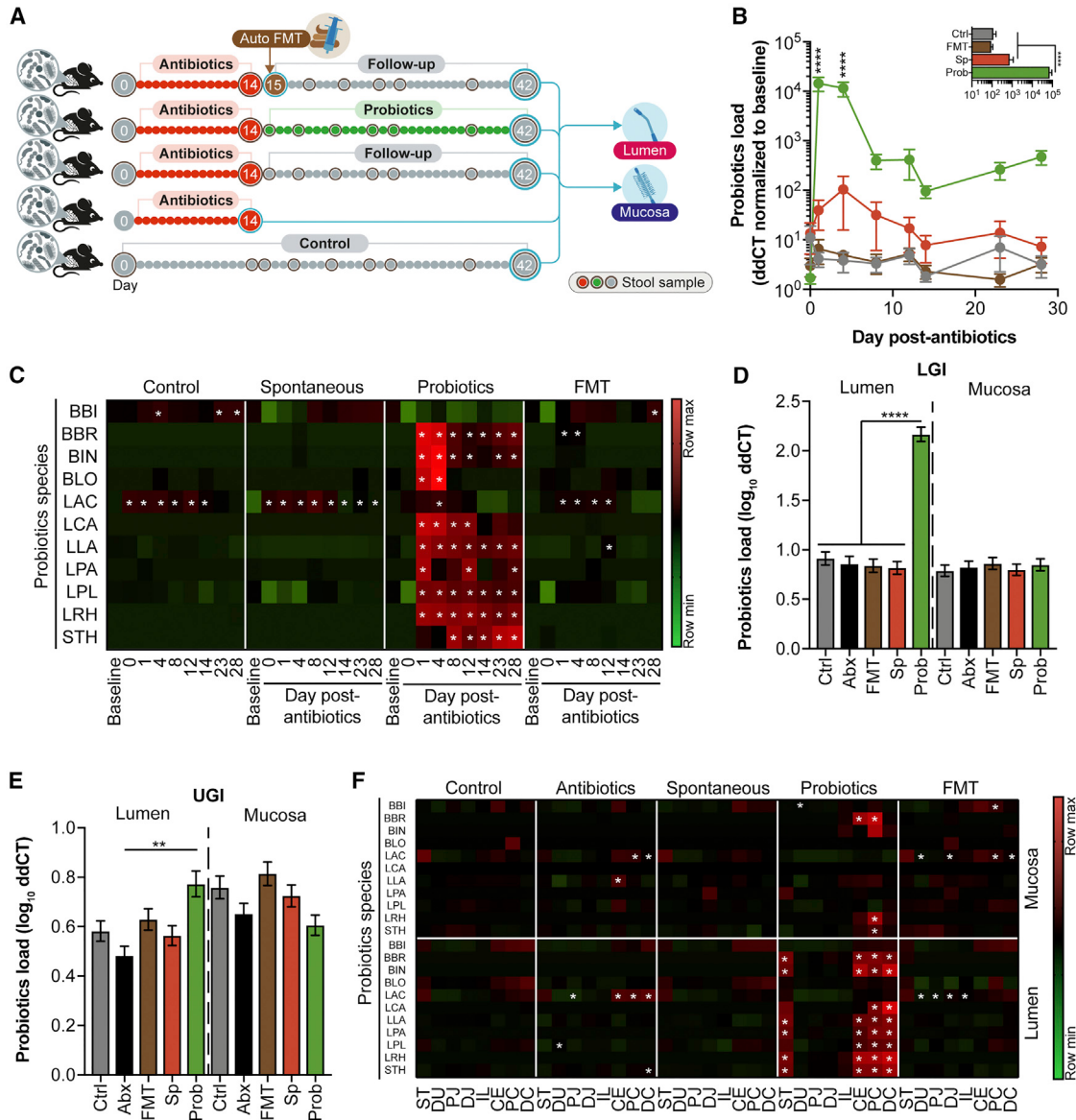


Figure 1. Probiotics Colonization in the Murine GI Tract following Antibiotic Treatment

Four groups of WT mice ($n = 10$) were treated for 14 days with ciprofloxacin and metronidazole in drinking water, after which one group was immediately dissected and three others were followed by either daily probiotics administration, a single aFMT with a pre-antibiotics fecal sample, or no intervention (spontaneous recovery). A fifth group ($n = 10$) did not receive antibiotics and remained untreated throughout. Absolute abundances of probiotics species were determined by qPCR in fecal samples collected at the various experimental stages or in GI tract tissues 28 days post antibiotics.

(A) Experimental design.

(B) qPCR-based fold change of pooled probiotics targets in fecal samples normalized to baseline (before antibiotics). *** $p < 0.0001$; two-way ANOVA and Tukey. Inset: incremental area under the curve describing the fold difference in cycle threshold (ddCT) between an indicated time-point and baseline, calculated from day 0 post antibiotics. *** $p < 0.0001$; Kruskal-Wallis and Dunn's.

(C) Same as (B) but for each probiotics species separately without normalization. * $p < 0.05$, two-way ANOVA and Dunnett.

(D and E) qPCR-based enumeration of pooled probiotics targets in tissues of the (D) LGI or (E) UGI. ** $p < 0.01$, *** $p < 0.0001$; Kruskal-Wallis and Dunn's.

(F) Same as (D) and (E) but for each probiotics species separately. * $p < 0.05$; two-way ANOVA and Dunnett. Symbols represent the mean, error bars represent SEM.

ST, stomach; DU, duodenum; PJ, proximal jejunum; DJ, distal jejunum; IL, ileum; CE, cecum; PC, proximal colon; DC, distal colon; Ctrl, control; Abx, antibiotics; Sp, spontaneous recovery; Prob, probiotics; BBI, *Bifidobacterium bifidum*; BBR, *Bifidobacterium breve*; BIN, *Bifidobacterium longum* subsp. *infantis*; BLO, *Bifidobacterium longum*; LAC, *Lactobacillus acidophilus*; LCA, *Lactobacillus casei*; LLA, *Lactococcus lactis*; LPA, *Lactobacillus casei* subsp. *paracasei*; LPL, *Lactobacillus plantarum*; LRH, *Lactobacillus rhamnosus*; STH, *Streptococcus thermophilus*. The experiment was repeated three times. See also Figure S1.

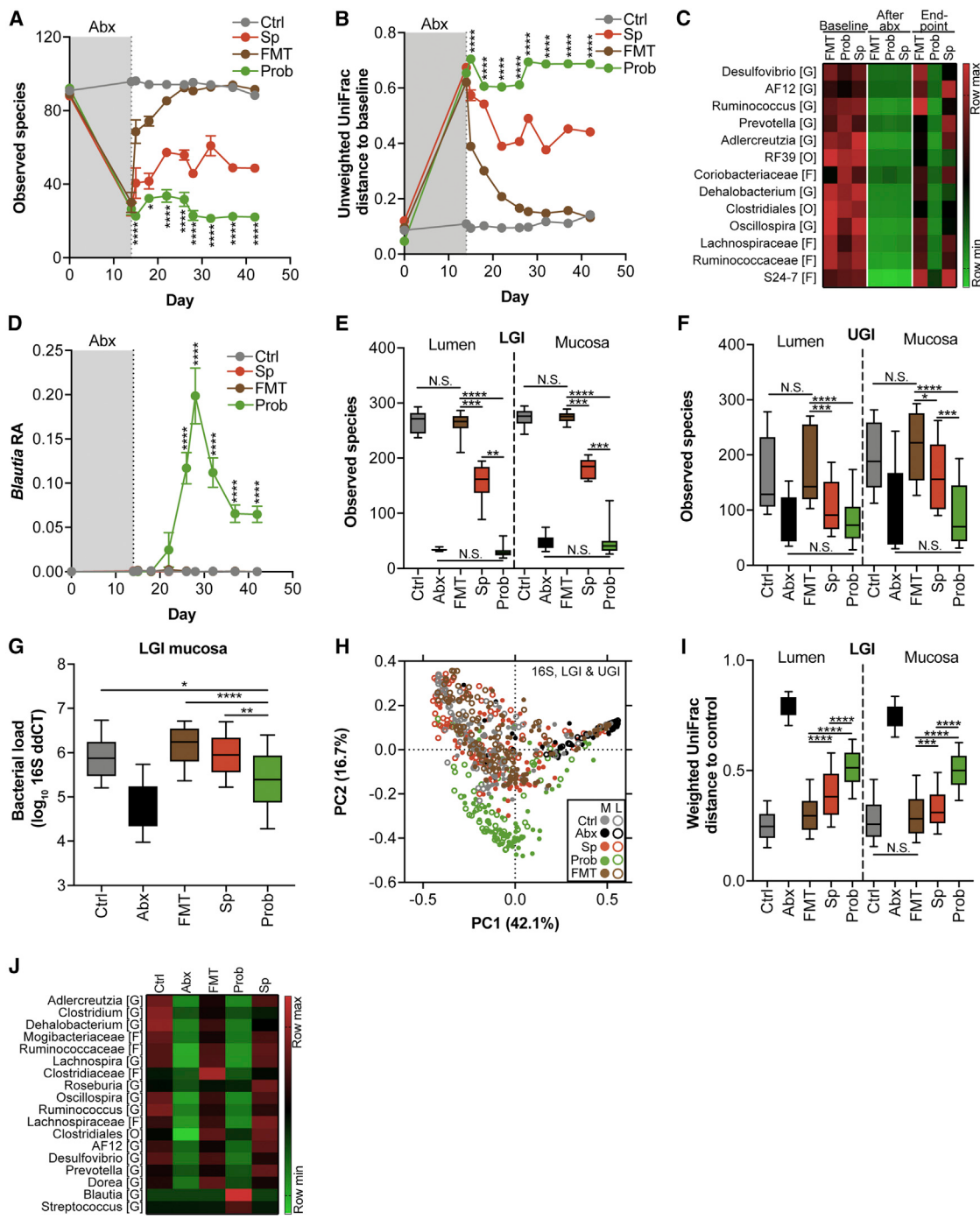


Figure 2. Probiotics Delay while aFMT Enhances the Reconstitution of the Murine Gut Microbiome following Antibiotic Treatment

16S rDNA-based comparison of post ciprofloxacin and metronidazole reconstitution in probiotics-treated mice (n = 10) compared to mice treated with aFMT (n = 10) and mice that did not receive post-antibiotics treatment and were followed up for 28 days (n = 10) or sacrificed immediately after antibiotics (n = 10) and no antibiotics controls (n = 10).

(A) Alpha diversity quantified as observed species. *p < 0.05, ***p < 0.0001 between probiotics and each of the other groups; two-way ANOVA and Dunnett.

(B) Unweighted UniFrac distances to baseline in feces. ***p < 0.0001 between probiotics and each of the other groups; two-way ANOVA and Dunnett.

(C) Genera significantly (false discovery rate [FDR]-corrected p < 0.05; Mann-Whitney) reduced by antibiotics in feces, which returned to baseline levels in aFMT and spontaneous recovery, but not in probiotics. In square brackets, the lowest taxonomic rank for which information was available; O, order; F, family; G, genus.

(D) Relative abundance of *Blautia* in fecal samples. ***p < 0.0001; two-way ANOVA and Dunnett.

(legend continued on next page)

GI lumen is contributed by the resident microbiome. This resistance is partially alleviated by antibiotics, although even after antibiotics pre-treatment, the tested probiotics demonstrated mild and sporadic mucosal presence, potentially reflecting lower colonization capacity of these human-compatible probiotics species in the murine gut mucosa.

Probiotics Delay and aFMT Improves the Post-Antibiotic Reconstitution of the Indigenous Murine Microbiome

We next determined the impact of the probiotic formulation on reconstitution of the indigenous murine fecal and mucosal gut microbiome community following antibiotic treatment. Expectedly, antibiotic treatment resulted in a dramatic reduction in stool alpha diversity (>66% reduction; [Figure 2A](#)) and general disruption of the fecal bacterial community structure as evident by unweighted UniFrac distances to baseline ([Figure 2B](#)). Of the three post-antibiotic interventions, aFMT was most efficient in restoring fecal bacterial richness to that observed in the control, with alpha diversity becoming indistinguishable to control within 8 days following aFMT ($p = 0.11$). In contrast, both probiotics and spontaneous recovery did not restore fecal alpha diversity to baseline levels 4 weeks following antibiotic cessation. Importantly, probiotics significantly delayed the return to baseline microbiome richness even compared to spontaneous recovery as evident in all tested time points ([Figure 2A](#)).

Delayed murine probiotics-induced microbiome reconstitution was also reflected in the kinetics of return to pre-antibiotics baseline fecal composition as expressed by UniFrac distances. Expectedly, all treatment groups were dramatically shifted from baseline stool composition upon antibiotic treatment. While aFMT returned to baseline by day 28 after antibiotic treatment ($p = 0.83$; [Figure 2B](#)), both the probiotics and spontaneous recovery groups failed to fully return to baseline within 4 weeks of antibiotics cessation, with microbiome in the probiotics-administered group featuring the slowest recovery rate ($p = 0.0001$). As a greater distance to baseline in the probiotics-supplemented group may be merely a result of new exogenous bacteria introduced into the microbiome, we repeated the measurement after removing the four probiotics genera from the analysis and renormalizing RAs to 1 and corroborated the greater distance to baseline of the probiotics-supplemented group, reflecting an impaired indigenous mucosal microbiome reconstitution in this group ([Figure S2B](#)). A pairwise comparison of fecal microbial composition between the last day of follow-up and baseline demonstrated 28 taxa significantly differentially represented in the probiotics group ([Figure S2C](#)) with a >10-fold increase in the abundance of *Blautia* and no significant increase in any of the probiotics genera. Fewer significant differences were observed in the spontaneous recovery (16 taxa; [Figure S2D](#)) and aFMT (6 taxa; [Figure S2E](#)) groups. Of all taxa

significantly reduced by antibiotics, 13 taxa belonging to 4 different phyla returned to baseline levels in both the aFMT and spontaneous recovery groups, but not in the probiotics group ([Figure 2C](#)). In contrast, five taxa were over-represented in the stool samples of the probiotics and significantly inversely correlated with alpha diversity: *Akkermansia*, *Vagococcus*, *Enterococcus*, *Blautia*, and *Lactococcus*. Of these, only *Blautia* bloomed exclusively in the probiotics group after antibiotics cessation ([Figure 2D](#)). Interestingly, macroscopic differences were noted between the ceca of probiotics-administered and spontaneously recovering mice, with the former being larger (representatives in [Figure S2F](#)) and significantly heavier ([Figure S2G](#)), reminiscent of germ-free mice or mice treated with broad-spectrum antibiotics.

Consistent with the findings in stool, the number of observed species in the probiotics group was comparable to the group dissected immediately after 2 weeks of antibiotics and significantly lower compared to the control, aFMT, and spontaneous recovery groups in both the lumen and the mucosa of the LGI ([Figure 2E](#)) and UGI ([Figure 2F](#)). No significant differences were noted between the aFMT and control groups in any of the regions, whereas the richness in the spontaneous group was in between that of aFMT and probiotics ([Figures 2E and 2F](#)). Reduced alpha diversity in the LGI of the probiotics group was at least partly due to a total reduction in LGI bacterial load ([Figure 2G](#)). In agreement, the UniFrac distance to control of the mucosal and luminal aFMT microbiome configuration was lower than that of the spontaneously recovering group, with the largest distance to control featured by the probiotics-administered group ([Figures 2H-2I and S2H](#)). As in stool, these colonization differences could not be explained by the mere presence of probiotics genera in probiotics-administered mice, as the result remained unchanged even if probiotics genera were excluded from the analysis ([Figures S2I and S2J](#)). Interestingly, microbiome composition of aFMT-treated mice was indistinguishable from controls both in the LGI and the UGI, suggesting that fecal microbiome was sufficient to recapitulate the distinct UGI microbiome ([Figure S2H](#)). Of the taxa significantly reduced in the LGI mucosa of the antibiotics group compared to control, 16 returned to control levels in both the aFMT and the spontaneous recovery groups, but not in the probiotics group, of which 11 belonged to the Clostridiales order; two genera (*Blautia* and *Streptococcus*) significantly bloomed exclusively in the probiotics group ([Figure 2J](#)). Four taxa predominant in the probiotics group had a high (Spearman $r < -0.6$) and significant ($p < 0.0001$) inverse correlation with the alpha diversity in the LGI mucosa: *Vagococcus*, *Akkermansia muciniphila*, *Blautia producta*, and *Enterococcus casseliflavus* ([Figure S2K](#)). These blooming taxa may thus play a role in probiotics-induced inhibition of microbiome reconstitution.

(E and F) Alpha diversity in tissues of the (E) LGI or (F) UGI. * $p < 0.05$, ** $p < 0.01$, *** $p < 0.001$, **** $p < 0.0001$; N.S., not significant; Kruskal-Wallis and Dunn's. (G) qPCR-based quantification of bacterial load according to 16S. Values are normalized to a detection threshold of 40. * $p < 0.05$, ** $p < 0.01$, *** $p < 0.0001$; Kruskal-Wallis and Dunn's.

(H) Weighted UniFrac principal-coordinates analysis (PCoA) of all tissues.

(I) Weighted UniFrac distances to control. *** $p < 0.001$, **** $p < 0.0001$; N.S., not significant; Kruskal-Wallis and Dunn's.

(J) Same as (C) but in tissues of the LGI mucosa. Symbols and horizontal lines represent the mean, error bars represent SEM or 10–90 percentile. Abx, antibiotics; LGI, lower gastrointestinal tissues; UGI, upper gastrointestinal tissues; Ctrl, control; Sp, spontaneous recovery; Prob, probiotics. See also [Figures S2](#) and [S3](#).

To ascertain that the delayed return to homeostatic indigenous microbiome configuration following probiotics treatment was not a unique feature of the studied vivarium, we performed the same set of interventions in mice housed in a different specific-pathogen-free (SPF) animal facility with distinct baseline fecal microbiome (26 taxa significantly differentially represented; [Figure S3A](#)). In this vivarium as well, aFMT induced a rapid indigenous microbiome post-antibiotic reconstitution as compared to watchful waiting, while the 11-strain probiotic treatment delayed the speed and magnitude of the recolonization process ([Figures S3B–S3K](#)).

Collectively, 4 weeks of spontaneous recovery following a broad-spectrum antibiotic treatment in mice partially restored baseline gut mucosal configuration and bacterial richness and load. Watchful waiting was superior—in its rate of induction of indigenous microbiome reconstitution—to consumption of probiotics, which demonstrated little improvement of the post-antibiotics microbiome configuration and delayed the restoration of homeostatic composition and richness of the pre-antibiotic gut mucosal microbiome. In comparison to both watchful waiting and probiotics administration, aFMT constituted the most efficient treatment modality, enabling rapid restoration of both upper- and lower-gut mucosal microbiome to homeostatic configuration following antibiotic treatment in mice.

Human Experimental Design

We next set out to determine how the 11-strain probiotics or aFMT would affect the post-antibiotic human luminal and mucosa-associated microbiome reconstitution. To this aim, we conducted a prospective longitudinal interventional study in 21 healthy human volunteers not consuming probiotics ([Table S1](#) and [STAR Methods](#)) who were given an oral broad-spectrum antibiotic treatment of ciprofloxacin and metronidazole at standard dosages for a period of 7 days ([Figure 3A](#)). Following antibiotic treatment, seven participants were followed by watchful waiting for spontaneous microbiome reconstitution, six participants received aFMT ([STAR Methods](#)), and eight participants received the aforementioned 11-strain probiotics preparation administered bi-daily for a period of 4 weeks ([Figure 3A](#)). Endoscopic examinations were performed twice in each of the 21 participants. A first colonoscopy and deep endoscopy were performed after completion of the week-long antibiotic course, thereby characterizing the post-antibiotics dysbiosis throughout the GI tract. A second colonoscopy and deep endoscopy were performed 3 weeks later (day 21) to assess the degree of gut mucosal and luminal reconstitution in each of the three treatment arms ([Figure 3A](#)). Multiple stool samples were collected at intervals indicated in [Figure 3A](#) up to 6 months from antibiotics cessation. In total, 337 luminal, 702 mucosal, and 557 stool samples, as well as 362 regional biopsies, were collected.

Probiotics in Antibiotics-Perturbed Humans Are Continuously Shed in Stool and Colonize the LGI Mucosa

Expectedly, antibiotic treatment in humans triggered a profound fecal microbial depletion ([Figure S4A](#)) and disruption of microbial community composition ([Figure S4B](#)) as observed in stool ([Figures S4C and S4D](#)), LGI mucosa ([Figures S4E and S4F](#)), and UGI mucosa ([Figure S4G](#)), with the latter region the least affected by antibiotics ([Figure S4H](#)). Compositional changes were

accompanied by alteration of microbiome function in the stool and LGI as assessed by shotgun metagenomic sequencing ([Figures S4I–S4K](#)).

Fecal 16S rDNA analysis demonstrated that all probiotics-related genera were found in stools prior to probiotics supplementation, and *Lactobacillus*, *Lactococcus*, and *Streptococcus* significantly expanded in RA following antibiotics treatment. All four probiotics genera remained significantly elevated compared to baseline during probiotics supplementation, though none were further elevated to the post-antibiotics levels. Following cessation of probiotic treatment, none of the genera remained significantly elevated compared to baseline ([Figures S5A–S5D](#)).

A fecal species-level metagenomic analysis (MetaPhiAn2) also demonstrated an antibiotics-induced expansion in RA of 6 of 11 species compared to baseline (BBI, BBR, BLO, LAC, LLA, and STH; [Figure S5E](#)), while during probiotic treatment, all species expanded compared to baseline, but only BBI and BLO reached statistical significance with this method ([Figure S5E](#)). A shotgun metagenomic sequencing strain-specific method ([Sharon et al., 2013](#)) identified one of the probiotic strains in a single baseline day in stool, two of the probiotics strains (different than the one appearing at baseline) during antibiotic treatment, and six of the pill-specific strains (BBI, BBR, BLO, LLA, LPL, and LRH) in multiple days during probiotics exposure. BBI, BLO, and BBR were also shed after cessation by the same participants ([Figure 3B](#)).

Fecal species-specific qPCR, the most sensitive method, revealed a significant fecal expansion during probiotics administration of the 11-probiotic species when considered together, with 7 of 11 species being significantly elevated from baseline when analyzed separately during consumption (BBR, BIN, LAC, LCA, LLA, LPL, and LRH; [Figure 3C](#)). This probiotic-species expansion was significant compared to both aFMT and spontaneous recovery ([Figures 3D and S5F](#)). Even 5 months after probiotics cessation, several probiotics species remained elevated in stools of the probiotics-supplemented group compared to baseline ([Figures 3D and S5F](#)).

Given the above continuous shedding in stool, we assumed that the post-antibiotic gut mucosal colonization of probiotics is also enhanced as compared to that observed during homeostasis ([Zmora et al., 2018](#)). 16S rDNA analysis of luminal and mucosal GI samples collected before and after 3 weeks of probiotics indicated no significant increases in the RA of probiotic genera in the GI lumen ([Figure S5G](#)) or mucosa ([Figure S5H](#)). MetaPhiAn2 analysis indicated that all probiotics species, except LPA, trended toward luminal expansion in RA from baseline, though none reached statistical significance ([Figure S5I](#)). In contrast, the mucosa of the TI and all LGI regions, except the rectum, featured significantly enhanced levels of probiotics species, stemming mostly from an elevation in BBI and BLO ([Figure S5J](#)). Consequently, improved post-antibiotic probiotics colonization was noted as compared to the naive probiotics-supplemented group ($p < 0.0001$; [Figure 3E](#)). Mucosal species-specific qPCR indicated a significant probiotics colonization of the gastric fundus; terminal ileum; ascending, transverse, and sigmoid colon; and the rectum ([Figure 3F](#)). Probiotics species were also significantly elevated in the ascending and transverse colon of the post-antibiotics spontaneous recovery group, while

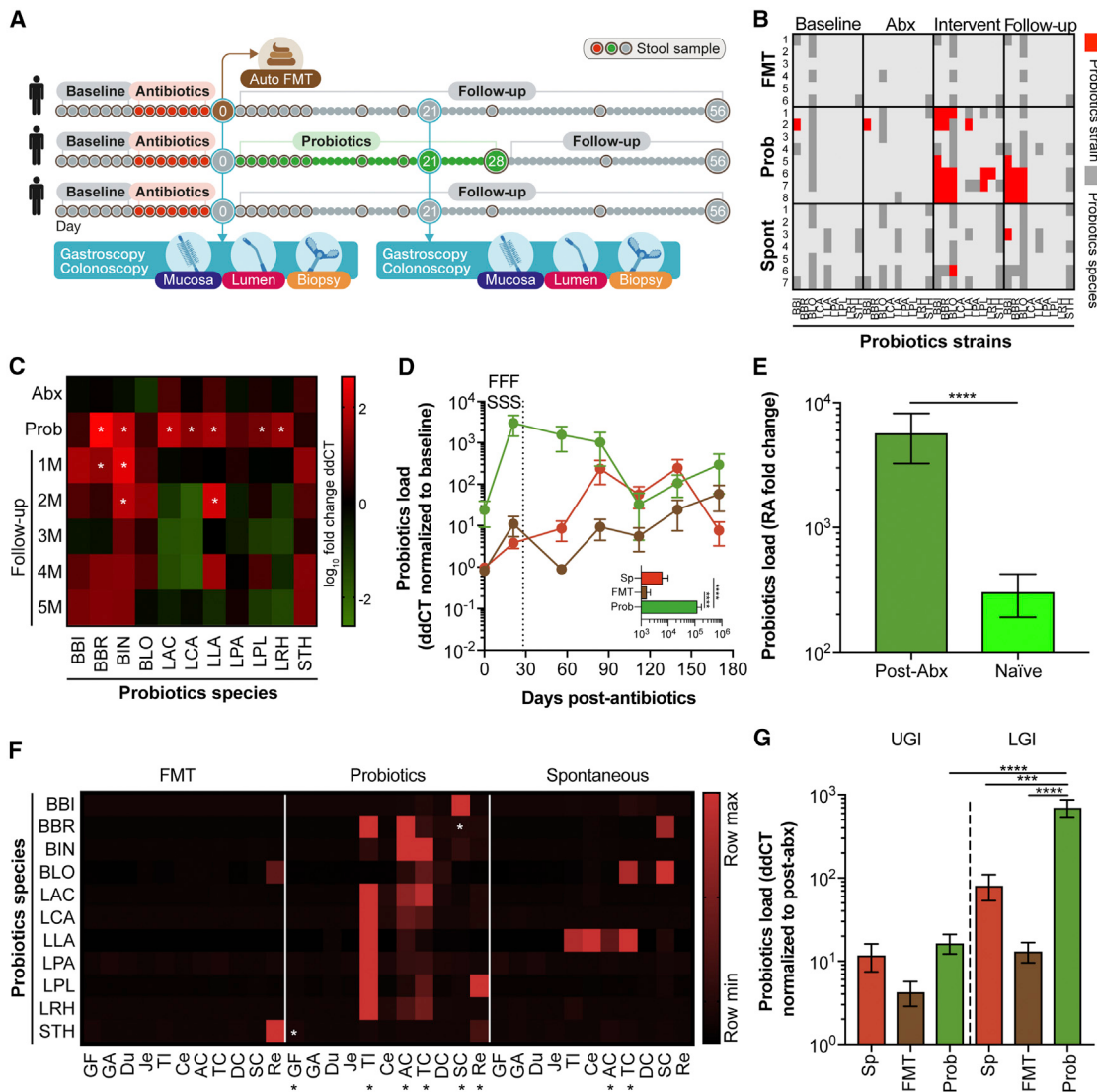


Figure 3. Probiotics Colonization in the Human GI Tract following Antibiotic Treatment

Three groups of humans were treated for 7 days with ciprofloxacin and metronidazole followed by either bi-daily probiotics pill administration ($n = 8$), aFMT of stool obtained before the antibiotics intervention ($n = 6$), or no intervention (spontaneous recovery; $n = 7$). Two endoscopic procedures were performed, and multiple stool samples were collected throughout the trial.

(A) Outline of the three arms of intervention in humans.

(B) Probiotics strain quantification in stool based on mapping of metagenomic sequences to unique genes that correspond to the strains found in the probiotics pill. Dark gray marks the presence of the probiotics species, and red marks the presence of the probiotics strains.

(C) qPCR quantification of probiotics species in stools from last day of antibiotics (Abx), day 19 of probiotics supplementation (Prob), and 1–5 months after cessation normalized to samples from the last baseline day before antibiotics. * $p < 0.05$; two-way ANOVA and Dunnett.

(D) Aggregated Probiotics load in stool in the three groups from the last day of antibiotics until 5 months of follow-up. SSS and FFF denote $p < 0.001$ versus spontaneous recovery or aFMT, respectively; two-way ANOVA and Tukey. Inset: iAUC from each group's baseline. *** $p < 0.0001$; Kruskal-Wallis and Dunn's.

(E) MetaPhlAn2-based aggregated quantification of probiotics species expansion (day 21 normalized to baseline) in tissues of individuals pre-treated with antibiotics or antibiotics-naïve (Zmora et al., 2018). **** $p < 0.0001$; Mann-Whitney.

(F) qPCR-based fold changes of probiotics species abundance in each mucosal tissue of each group. * p value < 0.05 ; two-way ANOVA for tissues and Dunnett per species per tissue relative to baseline.

(G) qPCR-based aggregated fold change in probiotics species abundance. *** $p < 0.001$, **** $p < 0.0001$; Kruskal-Wallis and Dunn's. Symbols represent the mean; error bars represent SEM.

GF, gastric fundus; GA, gastric antrum; Du, duodenum; Je, jejunum; TI, terminal ileum; Ce, cecum; AC, ascending colon; TC, transverse colon; DC, descending colon; SC, sigmoid colon; Re, rectum. BBI, *Bifidobacterium bifidum*; BBR, *Bifidobacterium breve*; BIN, *Bifidobacterium infantis*; BLO, *Bifidobacterium longum*; LAC, *Lactobacillus acidophilus*; LCA, *Lactobacillus casei*; LLA, *Lactococcus lactis*; LPA, *Lactobacillus paracasei*; LPL, *Lactobacillus plantarum*; LRH, *Lactobacillus rhamnosus*; STH, *Streptococcus thermophilus*. Sp, spontaneous recovery; Prob, probiotics. Abx, antibiotics, Intervent, intervention. See also Figures S4, S5, and S6.

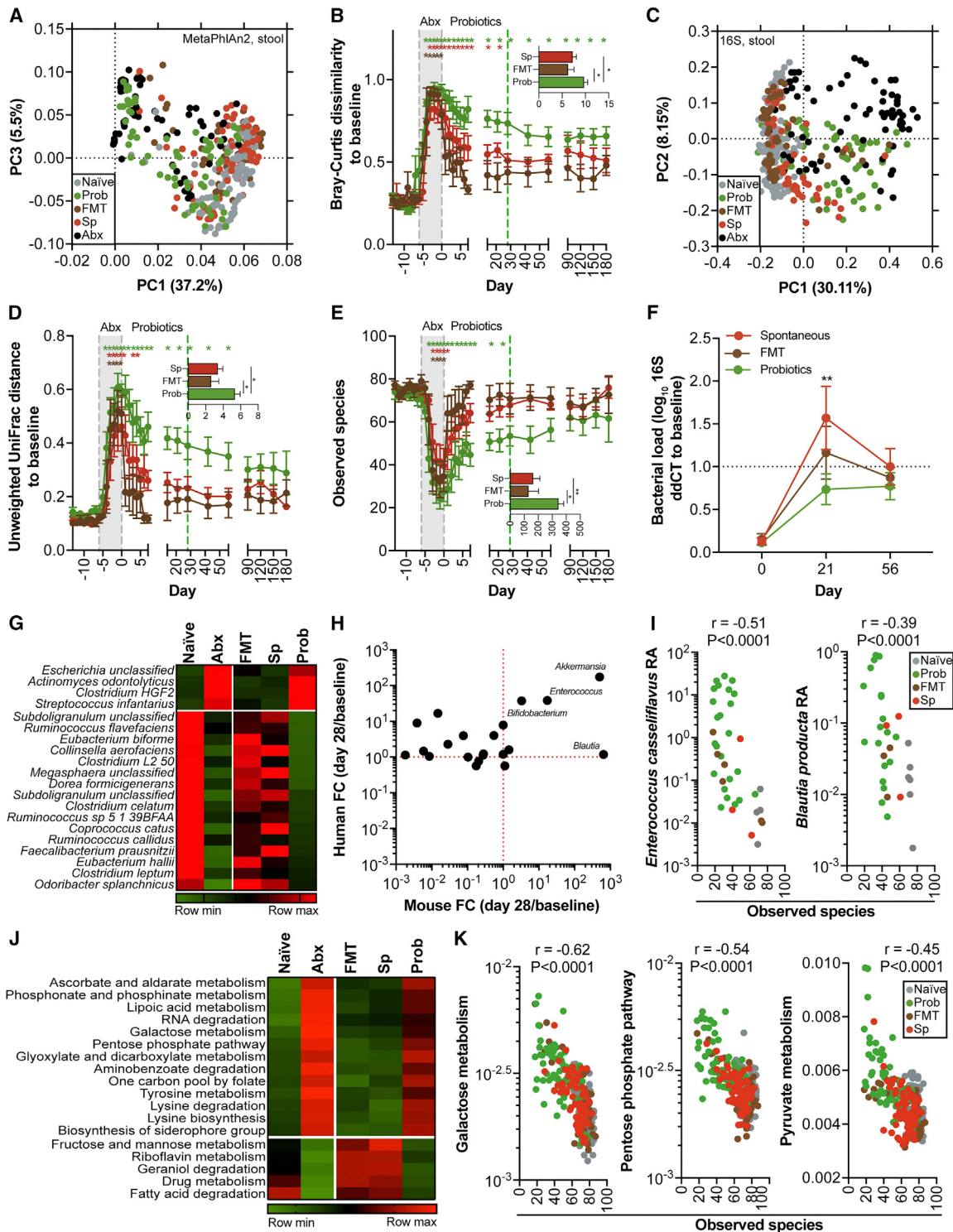


Figure 4. Probiotics Delay while aFMT Enhances the Human Fecal Microbiome Reconstitution to Baseline following Antibiotics Treatment

Stool samples collected during reconstitution from all treatment arms (starting from day 4 post antibiotics) were compared between groups and to their own baseline during antibiotics (Abx) and before antibiotics (Naive).

(A) MetaPhlAn2 species-based principal-component analysis (PCA) plot of stool samples collected during reconstitution in each of the treatment arms and during or before antibiotics.

(legend continued on next page)

no significant elevation was observed in the aFMT group (**Figure 3F**). On average, probiotics species expanded 8.7-fold more in the probiotics-supplemented group compared to spontaneous ($p = 0.0001$) and 53.9-fold compared to aFMT ($p < 0.0001$; **Figure 3G**).

To determine whether antibiotics-treated individuals feature a person-specific colonization permissiveness/resistance to probiotics, similar to our observations under homeostatic conditions (Zmora et al., 2018), we calculated qPCR-based individual fold changes in the probiotic load between the first and last days of probiotics supplementation (**Figure S6A**). In four participants, a significant >100-fold increase in mucosal probiotics load (aggregated for all targets) was observed (Wilcoxon $p < 0.02$). A fifth participant featured a milder but significant elevation. Three additional participants experienced a non-significant trend toward probiotics mucosal expansion. A probiotic-strain-specific shotgun-based validation analysis reflected this individualized pattern observed by qPCR and indicated that the colonizing strains originated from the supplemented pill (**Figure S6B**). The etiology and impact of these apparent inter-individual differences in post-antibiotic probiotic colonization merit further studies in larger cohorts.

Collectively in the antibiotics-perturbed human gut, reversal of colonization resistance to probiotics enabled incremental gut colonization by the tested exogenously administered probiotic strains, mainly in the large intestine, leading to long-term probiotic fecal shedding indicative of stable colonization and active proliferation. Probiotic species belonging to *Bifidobacterium* were colonized at higher levels compared to the other tested probiotics species.

Probiotics Delay While aFMT Improves the Post-Antibiotic Reconstitution of the Indigenous Human Fecal Microbiome

We next assessed the contribution of the three post-antibiotic treatment arms to reconstitution of the indigenous fecal microbiome in humans. We first utilized fecal MetaPhlAn2 species-based analysis to calculate the Bray-Curtis dissimilarity indices between stools collected during antibiotics treatment or during the reconstitution period to that of baseline stool microbiome configuration (**Figures 4A** and **4B**). Of note, dissimilarity from

baseline more than tripled during antibiotics treatment in all groups, reflecting the dramatic impact of antibiotics on stool microbiome configuration. aFMT-treated individuals were quickest to return to baseline configuration, with differences in stool composition compared to baseline disappearing as early as 1 day following aFMT (**Figure 4B**). In the spontaneous recovery group, significant differences in stool composition compared to baseline abated within 21 days of antibiotics cessation (**Figure 4B**). In contrast, probiotics-consuming individuals did not return to their baseline stool microbiome configuration by the end of the intervention period (day 28), and dysbiosis was maintained even 5 months after probiotics cessation, with all stool samples collected through day 180 remaining significantly different from baseline (two-way ANOVA and Dunnett $p < 0.01$; **Figures 4A** and **4B**). In addition to differences from baseline, probiotics-consuming individuals were also significantly distinct from the spontaneous recovery group through days 7–28 of the reconstitution. Consequently, the area under the probiotics-administered group reconstitution curve was significantly higher than aFMT and spontaneous recovery (**Figure 4B**). As in mice, the distinct microbiome composition could not be explained by the mere presence of probiotics species in probiotics-consuming individuals, as the result remained unchanged even if probiotics species were excluded from the analysis and RAs were renormalized (**Figures S6C** and **S6D**). Delayed reconstitution in probiotics-consuming individuals was also observed by 16S-rDNA-based unweighted UniFrac distances (**Figures 4C** and **4D**) even when probiotics genera were omitted from the analysis (**Figures S6E** and **S6F**).

We next quantified species and functional KEGG orthologs (KOs) that were more than 2-fold distinct in their fecal abundances between baseline (pre-antibiotics) and the end of reconstitution in the three arms. aFMT featured the fewest number of fecal species distinct between baseline and endpoint (29 species; **Figure S6G**), while probiotics had the most fecal species distinct between baseline and endpoint (96; **Figure S6H**)—almost double than those observed during spontaneous recovery (51; **Figure S6I**). Three taxa significantly reverted to naive levels by aFMT, but not by spontaneous recovery (*Alistipes shahii*, *Roseburia intestinalis*, and *Coprococcus*). Microbiome function, as determined by fecal KOs, displayed the same

(B) Bray-Curtis dissimilarity to baseline stool samples of each participant (mean of a group is plotted) throughout the experiment. Colored asterisks indicate any $p < 0.05$ versus baseline for clarity; two-way ANOVA and Dunnett. Inset: area under the post-antibiotics reconstitution curve for each group. * $p < 0.05$; Kruskal-Wallis and Dunn's.

(C) Same as (A) but with 16S-based unweighted UniFrac distances.

(D) Same as (B) but with 16S-based unweighted UniFrac distances.

(E) Same as (B) but with observed species.

(F) 16S qPCR-based quantification of bacterial load normalized to baseline before antibiotics. ** $p < 0.01$ probiotics versus spontaneous; two-way ANOVA and Tukey.

(G) Intersection analysis of species significantly reduced or increased compared to baseline by antibiotics and reverted by aFMT and spontaneous recovery, but not by probiotics. Listed are species with minimal coefficient of variation between aFMT and spontaneous recovery and maximal between probiotics and the other two arms.

(H) Fold change (FC) between the last day of probiotics and baseline in humans and mice of genera detected in feces of both organisms.

(I) Top species significantly anti-correlated with alpha diversity in feces. Samples are colored according to group. Significance and r values according to Spearman.

(J) Same as (G) but for KEGG pathways.

(K) Same as (I) but with KEGG pathways.

Symbols represent the mean; error bars represent SEM. See also **Figure S6** and **Table S2**.

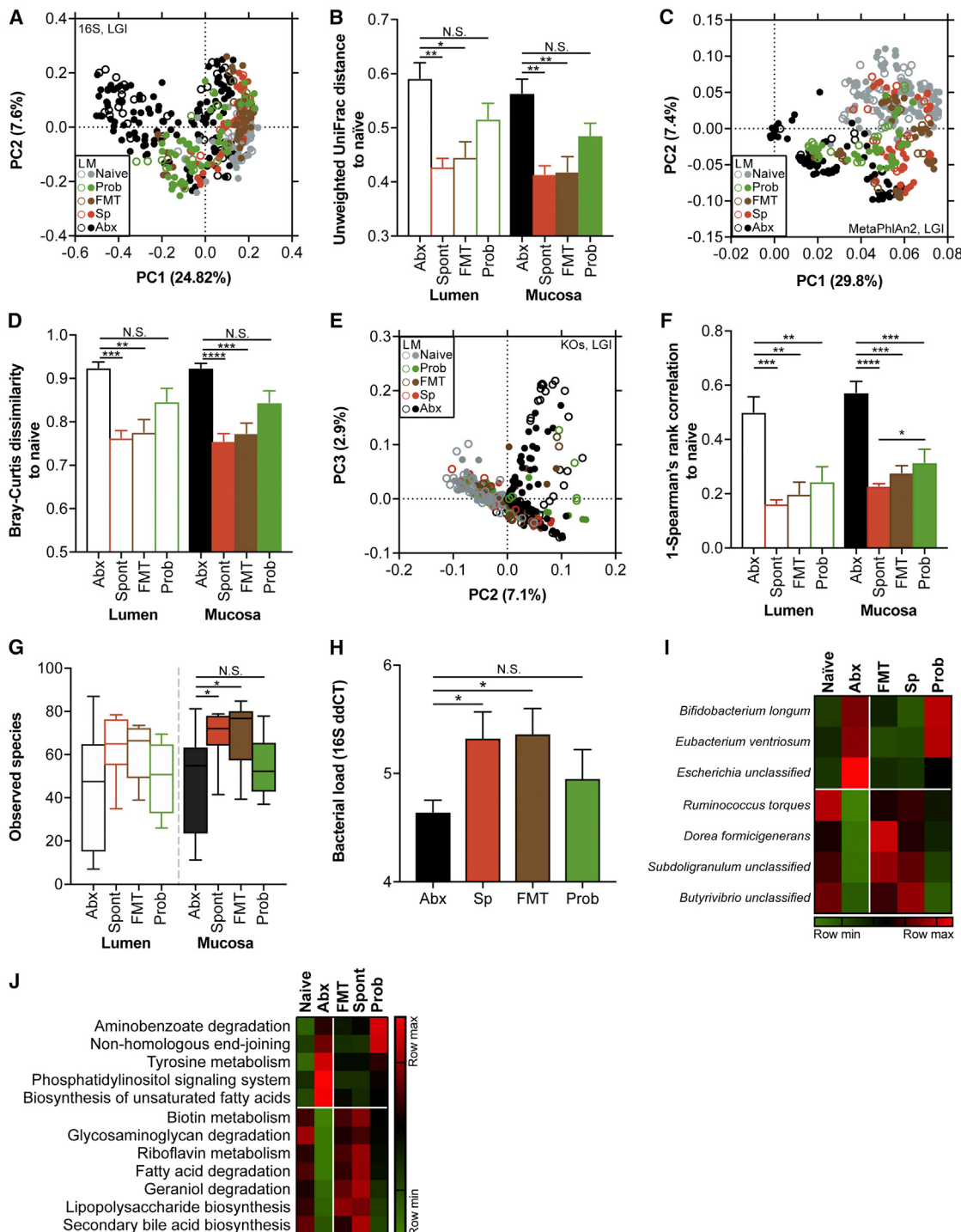


Figure 5. Probiotics Delay while aFMT Enhances the Human Gut Mucosal and Luminal Microbiome Reconstitution to Baseline following Antibiotics Treatment

Lumen and mucosa samples collected three weeks post antibiotics in each of the study arms were compared to samples collected on the last day of antibiotics (Abx) and samples from antibiotics-naïve individuals.

(A) PCoA plot demonstrating different reconstitution patterns 3 weeks after antibiotics treatment in subjects receiving probiotics after antibiotics therapy in terms of 16S rDNA sequencing.

(B) Unweighted UniFrac distance from antibiotics-naïve mucosal samples. Significance according to Mann-Whitney.

(C) Same as (A) but PCA based on MetaPhlAn2 species abundances.

(legend continued on next page)

pattern (9 KOs in aFMT, 123 in probiotics, and 17 in spontaneous recovery; Figures S6J–S6L, respectively). Importantly, following antibiotics treatment, the number of observed species in feces was halved but was restored in both the aFMT and the spontaneous recovery groups within 1 and 2 days, respectively (Figure 4E). In contrast, the alpha diversity remained significantly low and did not return to baseline in the probiotics group throughout the intervention period (two-way ANOVA and Dunnett $p < 0.05$; Figure 4E), with the alpha diversity reconstitution curve remaining lower compared to its own baseline, as well as aFMT or spontaneous, up to 5 months post probiotics cessation (Figure 4E). Likewise, fecal bacterial load failed to return to baseline after 3 weeks of probiotics supplementation, as compared to both aFMT and spontaneous recovery (Figure 4F), and remained lower than baseline 1 month after probiotics supplementation ceased.

Of the species altered in fecal RA by antibiotics, we identified 20 that returned to baseline levels in the aFMT and spontaneous recovery groups, but not in the probiotics group (Figure 4G). As in the mouse, the majority of the probiotics-inhibited species belonged to the Clostridiales order. A comparison between the probiotic-induced taxonomic changes in humans and mice indicated that four taxa—*Enterococcus*, *Akkermansia*, *Bifidobacterium*, and *Blautia*—bloomed after probiotics supplementation in both species (Figure 4H). To assess which of the blooming taxa may be involved in microbiome inhibition, we correlated 16S- and MetaPhlAn2-based abundances with alpha diversity. 14 genera and 107 species were significantly inversely correlated with alpha diversity, including the majority of probiotics species (excluding LPA and STH), as well as *E. casseliflavus* and *B. producta* that were also significantly inversely correlated with alpha diversity in the mouse LGI mucosa (Figures 4I and S2K and Table S2). Likewise, we identified multiple pathways that returned to their pre-antibiotics state in aFMT and spontaneous recovery, but not in probiotics (Figure 4J). 37 KOs and 60 pathways, the majority of which relate to metabolism, were significantly inversely correlated with alpha diversity in stool (Table S2). The highest anti-correlation was with galactose metabolism, which, along with additional pathways, may be related to lactate production and consequently microbiome inhibition by the probiotic species that bloom in the fecal samples (Figure 4K).

Together, while probiotics species colonized the mucosa of the antibiotics-perturbed human gut, they delayed the stool microbiome compositional, functional, and diversity-related reconstitution toward a pre-antibiotic configuration. This delayed fecal reconstitution persisted even 5 months after

probiotic cessation. In contrast, aFMT induced a rapid and nearly complete fecal microbiome reconstitution as compared to either the watchful waiting or probiotics-administered groups.

Probiotics Delay the Post-Antibiotic Reconstitution of the Indigenous Human Mucosal Microbiome

We next assessed whether the above inverse probiotics- and aFMT-induced impacts on stool microbiome reconstitution could be documented at the gut mucosa level. We focused on the LGI, given the preferential probiotic post-antibiotic colonization at this region (Figures 3G and S5I and S5J). Both 16S-rDNA (Figures 5A and 5B) and MetaPhlAn2-based (Figures 5C and 5D) analyses demonstrated that the aFMT and spontaneous recovery LGI luminal and mucosal configurations were significantly more similar to that of naive non-antibiotics-treated controls than to the antibiotics-perturbed configuration. In contrast, the probiotics LGI configuration remained similar to the antibiotics-perturbed configuration (Figures 5A–5D). The greater distance from the naive configuration of the probiotics group was not merely reflecting the presence of the probiotics species, as removal of the probiotics genera (Figures S7A and S7B) or species (Figures S7C and S7D) from the distance analysis maintained the aforementioned pattern. The function of the microbiome in KOs (Figures 5E and 5F) and pathways (Figures S7E and S7F) also mirrored the delayed probiotics-associated restoration of the indigenous mucosal LGI microbiome. As in stool, the LGI mucosa of the probiotics group displayed a lower alpha diversity, which was comparable to that observed immediately after antibiotics (Figure 5G) and reflected also in LGI mucosa bacterial load (Figure 5H). As in stool, multiple species (Figure 5I) and microbial pathways (Figure 5J) were altered by antibiotics and reverted to homeostatic levels by aFMT and spontaneous recovery, but not by probiotics, with all the inhibited species belonging to Clostridiales (Figure 5I). 8 genera, 62 species, 80 KOs, and 26 pathways were significantly anti-correlated with alpha diversity in the LGI mucosa, with high similarity in species (69%) and pathways (84%) between stool and mucosa (Table S2).

Collectively, enhanced post-antibiotic probiotics colonization in the LGI mucosa was associated with a compositional and functional persistence of post-antibiotic dysbiosis reflected in both stool and LGI lumen and mucosa. This delayed return of the indigenous gut microbiome toward pre-antibiotic microbiome composition and function is in line with our observations in mice (Figures 2, S2, and S3), suggestive of a global mechanism of interaction between the indigenous microbiome and exogenous probiotics across host species.

(D) Same as (B) but with Bray-Curtis dissimilarity.

(E) Same as (A) but PCA based on KO abundances.

(F) Same as (B) but with KO abundances-based Spearman correlation.

(G) Observed species in the LGI lumen and mucosa on day 21 post antibiotics. Significance according to Mann-Whitney.

(H) Bacterial load in the LGI mucosa as determined by 16S qPCR. CT values are normalized to a detection threshold of 40. Significance according to Kruskal-Wallis and Dunn's.

(I) Intersection analysis of species significantly reduced or increased compared to baseline by antibiotics and reverted by aFMT and spontaneous recovery, but not by probiotics. Listed are species with minimal coefficient of variation between aFMT and spontaneous recovery and maximal between probiotics and the other two arms.

(J) Same as (I) but for KEGG pathways. Symbol and horizontal bar represent the mean; error bars represent SEM; * $p < 0.05$, ** $p < 0.01$, *** $p < 0.001$, **** $p < 0.0001$. N.S., non-significant. See also Figure S7 and Table S2.

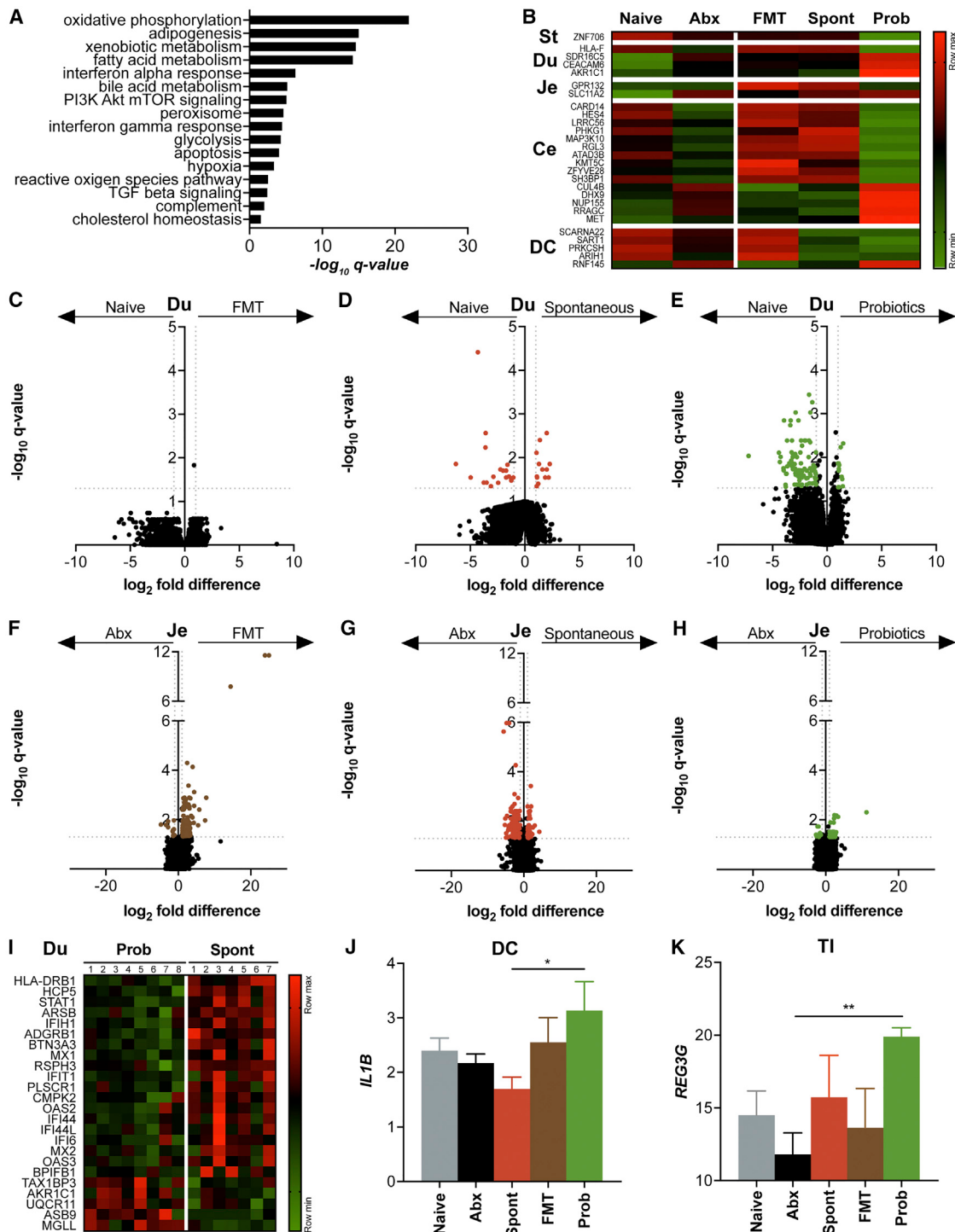


Figure 6. Probiotics Delay while aFMT Enhances the Post-Antibiotic Reconstitution of the Human Gut Transcriptome

(A) Pathways that are significantly affected by antibiotics in the descending colon. FDR-corrected $p < 0.05$.

(B) Genes that are significantly altered by antibiotics compared to the naive state and reverted by aFMT and spontaneous recovery, but not by probiotics in every region.

(C–E) Quantification of genes in the duodenum distinct between the naive state and (C) post-FMT, (D) post spontaneous recovery, or (E) post probiotics.

(F–H) same as (C)–(E) but comparing to the post-antibiotics transcriptome in the jejunum.

(I) Genes significantly different after 3 weeks of post-antibiotics and spontaneous reconstitution or probiotics in the duodenum.

(legend continued on next page)

Reversion of Antibiotics-Associated GI Transcriptomic Landscape Is Delayed by Probiotics

Given the differential impact of probiotics and aFMT, as compared to watchful waiting, on the recovery of mucosal gut microbiome composition and function, we next sought to characterize the effect of the three post-antibiotics interventions on the host. To this aim, we performed a global gene expression analysis through RNA sequencing of transcripts collected from stomach, duodenum, jejunum, terminal ileum, cecum, and descending colon biopsies immediately after antibiotics treatment and 3 weeks later into the three post-antibiotic interventions (Figure 3A). Of note, antibiotics affected the transcriptional landscape across the GI tract, with the majority of differences between naive and antibiotics state observed in the descending colon (Figure 6A). Importantly, restoration of the antibiotics-naive host transcriptional landscape by the three post-antibiotics intervention arms mirrored our findings in the microbiome, as multiple genes across the GI tract that were significantly affected by antibiotics were reverted toward homeostatic expression levels by spontaneous recovery and aFMT, but not by probiotics (Figure 6B). When compared to the global naive (non-antibiotics-exposed) transcriptional state, duodenal transcriptomes of the post-aFMT group featured the least amount of significantly differentially expressed genes (Figure 6C), followed by the spontaneous recovery group (Figure 6D), while the duodenal transcriptional landscape was most distinct from the naive state in the probiotics group (Figure 6E). In agreement, jejunum from the probiotic groups featured the greatest similarity to the post-antibiotic transcriptional state as compared to the transcriptome of the aFMT or spontaneous recovery groups (Figures 6F–6H). The highest number of significant differences between the probiotics and spontaneous recovery groups was observed in the duodenum, including multiple genes belonging to the interferon-induced proteins (IFIs) that were under-expressed in probiotic consumers (Figure 6I). Interestingly, probiotics led to an elevation in the transcript levels of inflammatory mediators and regulators of anti-microbial peptide secretion, such as *IL1B* (Figure 6J), and of some anti-microbial peptides, such as *REG3G* (Figure 6K), potentially contributing to the inhibition of indigenous commensals such as Clostridiales.

Probiotics-Secreted Molecules Inhibit Human Microbiome *In Vitro* Growth

Finally, we explored potential direct probiotic-mediated mechanisms contributing to the inhibition of indigenous microbiome restoration. To this aim, we utilized a host-free, contact-independent system of probiotics-human-microbiome culture. We began by culturing the probiotics pill content in five selectively enriching growth media, differentially supporting the growth of each of the four genera composing the probiotics consortium (Figure 7A). Following 24 hr of anaerobic culture, supernatants from each of the five growth conditions were added to a lag-phase culture of fresh naive human fecal microbiome under anaerobic conditions.

Optical density (OD) of the microbiome culture, measured after 8 hr, indicated that soluble factors in the de Man, Rogosa, and Sharpe medium (MRS)-probiotics culture supernatant (which mostly supports the growth of *Lactobacillus*) inhibited the growth of the naive human microbiome (Figure 7B). This inhibitory effect was not merely due to acid production by the probiotic bacteria, as the probiotics filtrate had an additive inhibitory effect to that of a comparably acidified, non-bacterial-exposed medium (pH 4; Figure 7C). To corroborate that *Lactobacillus* was indeed the microbiome-inhibitory probiotic, we collected supernatants from (1) an MRS anaerobic culture supernatant of a probiotic pill content, (2) an MRS anaerobic culture supernatant of a mix of the five *Lactobacillus* species present in the pill, and (3) a non-cultured MRS medium acidified to the levels measured with the other two cultures (pH 4; Figure 7D). The three supernatants were then cultured with a naive human microbiome under anaerobic conditions. Importantly, a significant growth inhibition was induced by both probiotics and *Lactobacillus* supernatants as compared to acidified MRS, suggestive of secreted *Lactobacillus* factors promoting the inhibitory effects (Figure 7D). 16S rDNA analysis of the filtrate-supplemented human microbiome cultures following 11 hr of culturing indicated that these soluble factors significantly reduced the number of observed species (Figure 7E) and modulated community structure (Figures 7F and 7G). This resulted in reduced levels of *Prevotella* and several taxa belonging to Clostridiales (Figure 7H), in line with our observations with *in vivo* probiotic administration.

DISCUSSION

In this study, we examined in both mice and humans the effects of post-antibiotic consumption of an 11-species probiotic preparation or of aFMT on gut mucosal microbiome community structure. We utilized an invasive post-antibiotic endoscopic characterization of the gut mucosa and demonstrated that the homeostatic microbiome-mediated colonization resistance to the administered probiotics is at least partially overcome upon antibiotics treatment, resulting in an improved probiotics colonization of the depleted gut mucosal layer at its entirety—in humans more than in mice. Importantly, in both mice and humans, we demonstrate that enhanced post-antibiotic probiotic colonization comes at a tradeoff of delayed indigenous microbiome and host mucosal transcriptome reconstitution to a homeostatic configuration as compared to either watchful waiting or aFMT. In contrast, aFMT results in rapid and nearly complete reconstitution of the gut mucosal microbiome configuration and host gut transcriptome.

Our study highlights several important points. First, it provides direct evidence that colonization resistance to the administered probiotics in mice, and the person-specific colonization resistance to the administered probiotics in humans (Zmora et al., 2018), were contributed by the indigenous gut microbiome. In inbred mice featuring a relatively uniform microbiome

(J) Normalized number of transcripts for *IL1B* in the descending colon after 3 weeks reconstitution.

(K) Same as (J) but for *REG3G* in the ileum.

St, stomach; Du, duodenum; Je, jejunum; TI, terminal ileum; Ce, cecum; DC, descending colon. * $p < 0.05$, ** $p < 0.01$; Kruskal-Wallis and Dunn's. Prob, probiotics, Spont, spontaneous recovery. Horizontal lines represent the mean; error bars represent SEM.

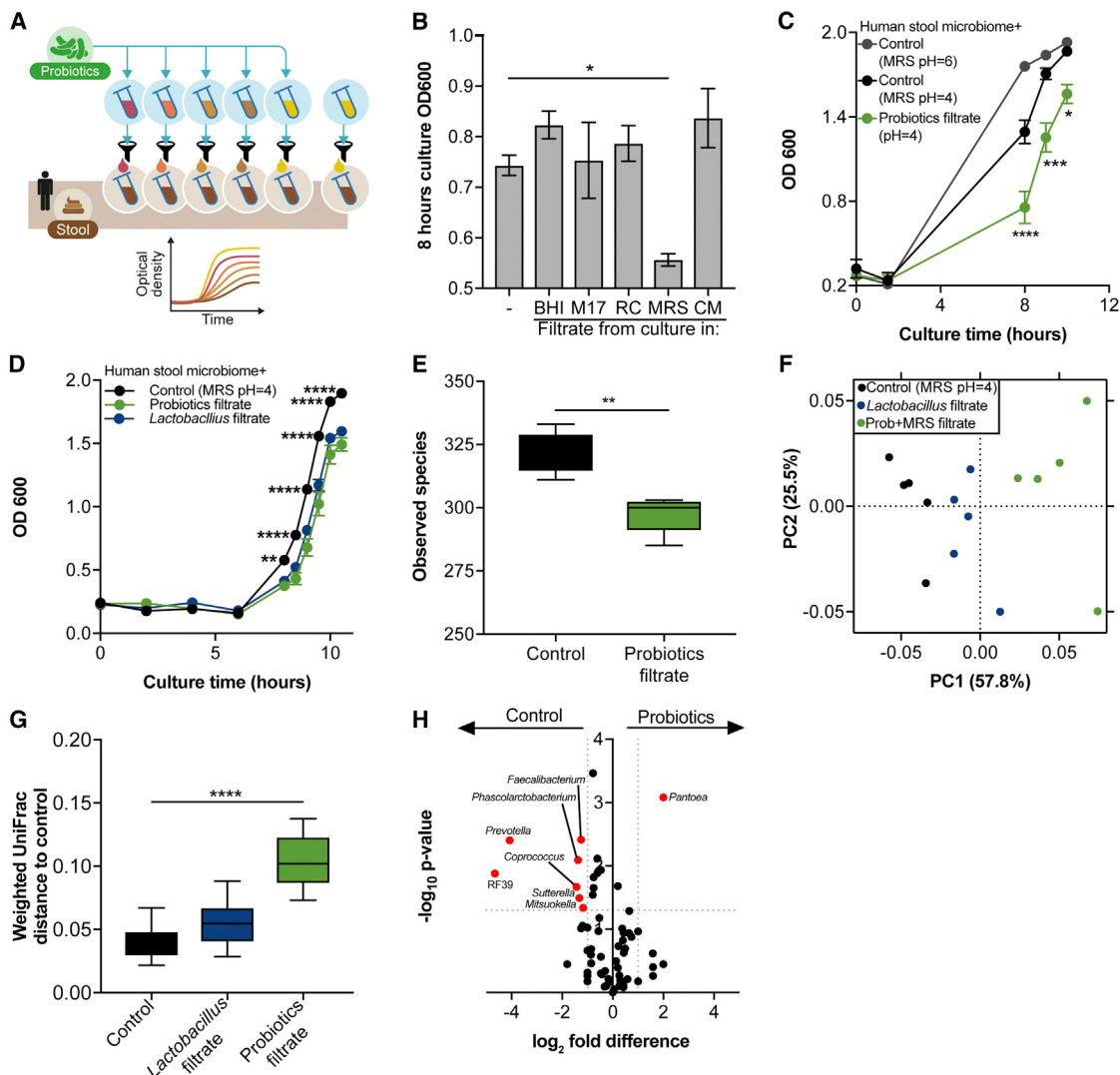


Figure 7. Probiotics-Associated Soluble Factors Inhibit the Human Fecal Microbiome

The content of a probiotics pill was cultured in various media to enhance differential growth. The supernatant was filtered using a 0.22-µm filter and added to a lag-phase human fecal microbiome culture in BHI, and growth was quantified by optical density.

(A) Experimental design.

(B) OD measured after 8 hr of fecal culture with filtrates from the various probiotics cultures. *p < 0.05; one-way ANOVA and Dunnett. -, fecal culture with PBS (no filtrate).

(C and D) OD-based growth curves of fecal microbiome cultured with probiotics-MRS filtrate or sterile acidified MRS. These two conditions are additionally compared to either (C) non-acidified sterile MRS or (D) a filtrate mixed from pure cultures of each of the five *Lactobacillus* species present in the pill. *p < 0.05, **p < 0.01, ***p < 0.001, ****p < 0.0001; two-way ANOVA and Tukey.

(E) Alpha diversity based on 16S rDNA of cultures from (D) harvested after 11 hr. **p < 0.01; two-tailed t test.

(F and G) Weighted UniFrac distances of samples from the three conditions in (D) harvested after 11 hr. ***p < 0.0001; Kruskal-Wallis and Dunn's.

(H) Taxa under or over-represented in the culture with probiotics filtrate compared to acidified MRS. In red, Mann-Whitney p < 0.05. Each condition was represented by 3–5 tubes. The experiment was repeated three times. Symbol and horizontal bars represent the mean; error bars represent SEM or 10–90 percentile.

configuration, the absence of a microbiome under extreme germ-free condition (Zmora et al., 2018) resulted in preferential and sustained probiotic colonization, pointing toward the indigenous microbiome as a major driver of colonization resistance to these administered strains in the murine gut environment. Less extreme microbiome depletion by broad-spectrum antibiotic treatment in mice only mildly improved probiotics coloni-

zation, suggesting that human compatibility of the examined probiotic strains, or other uneradicated microbial factors, may contribute to murine colonization resistance in this setting, in line with a previous report (Grazul et al., 2016). Humans, in contrast, feature highly diverse microbiome configurations (Yatsunenko et al., 2012; Zeevi et al., 2015), driving an individualized capacity of homeostatic colonization of the 11 probiotic strains

(Maldonado-Gómez et al., 2016; Goossens et al., 2006; Zmora et al., 2018). Antibiotic perturbation in humans, followed by administration of the 11 human-compatible probiotic strains, resulted in a marked mucosal colonization enhancement. Even then, only *Bifidobacterium* strains persisted following probiotics cessation in some of the individuals—an observation previously suggested to stem from adaptations of the genus to the human gut (Maldonado-Gómez et al., 2016). Deciphering the microbial contributors and associated molecular mechanisms orchestrating colonization resistance to exogenous bacteria present during homeostasis and lost during antibiotic treatment may enable harnessing these mechanisms toward better long-term colonization efficacy of probiotics treatment in different clinical contexts.

Second, our study highlights an important previously unappreciated tradeoff in which improved probiotic gut mucosal colonization under disruptive antibiotic conditions led to a markedly delayed indigenous gut mucosal reconstitution in terms of composition, function and bacterial load, and prolonged dysbiosis that lasted at least 5 months following the cessation of probiotic exposure. While our study is not aimed or powered to assess the effectiveness, or lack thereof, of probiotics in ameliorating post-antibiotics clinical symptoms, we demonstrate that their putative “placeholder” effect may come at a price of significant prolongation of dysbiosis and delayed recolonization of the indigenous microbiome, resulting in altered reversion of the host gut transcriptome toward homeostatic configuration. This probiotic-induced “adverse effect” may be important in light of multiple observations linking antibiotics-associated dysbiosis and lower microbial diversity with increased susceptibility to a myriad of chronic and infectious diseases (Vangay et al., 2015). The duration, extent, and long-term health consequences of probiotics-induced delayed endogenous microbiome and host transcriptome reconstitution—and whether they occur with other probiotics not tested in our study—merit further studies.

Given this probiotics effect, it would be critically important to further elucidate probiotics-induced factors contributing to the inhibition of indigenous microbiome reconstitution. Synthesis of our human, mouse, and *in vitro* data points to an antagonistic activity of some probiotics species and related blooming lactic acid bacteria such as *Enterococcus* and *Vagococcus*, as well as *B. producta* and *Actinomyces odontolyticus*, against the native commensal microbiome, potentially mediated by their previously established anti-microbial activity (Caballero et al., 2017; Franz et al., 2007; Cotter et al., 2013; Franker et al., 1977) that was overlooked in the context of commensals. Genetic or pharmacologic inhibition of such factors may promote better post-probiotic microbiome recovery, thereby complementing probiotics use.

Third, our study highlights the potential advantage of aFMT as an effective means of minimizing the post-antibiotics gut mucosal microbiome “nadir” period. Indeed, aFMT, constituting an inherently compatible personalized stool microbiome configuration, was associated with a markedly improved rate of indigenous microbiome colonization and reversion of the host gut transcriptome toward a homeostatic configuration as compared to the tested probiotic preparation or watchful waiting. As such, aFMT may provide a rapid post-antibiotic protec-

tion from pathogen and pathobiont engagement with the host during the critical and vulnerable post-antibiotic period without exposing the host to a delayed indigenous microbiome recolonization and its potential long-term consequences. Of note, while aFMT is increasingly studied in various clinical contexts (Koette et al., 2017) and promoted through non-medical channels and bio-banking entities (Smith et al., 2014; Terveer et al., 2017), we expect its widespread use as an “antibiotics adjuvant” to be technically challenging, as it necessitates long-term stool storage, extensive pill production, and rapid delivery to patients. An alternative, scientifically sound aFMT replacement modality would necessitate characterization of a person-specific “core gut mucosal microbiome function” enabling the generation of individualized bio-active commensal probiotic consortia providing post-antibiotics mucosal protection and core microbiome function. We expect such a highly defined, individual-tailored modality to enable improved clinical efficacy and reproducibility of probiotic use while minimizing the related potential consequences of indiscriminate probiotics colonization. This “personalized probiotics” approach merits further research.

Our study features several important limitations. We tested, in mice and humans, a single combination of broad-spectrum antibiotics and one (albeit diverse) orally administered probiotics mixture. Other combinations of antibiotics, probiotics, and treatment routes and timings merit further studies. Furthermore, our study was conducted in healthy adults voluntarily consuming antibiotics as part of this trial and was not aimed or powered to assess clinical responses to probiotics. Results may differ in the context of disease and in extreme age groups such as the pediatric population, in which the microbiome configuration has yet to stably mature and stabilize, or the geriatric population, which features other distinct microbiome changes.

Notwithstanding these limitations, our study demonstrates, in one empiric multi-strain probiotic preparation, that the presumed probiotic-induced protection from antibiotic-associated adverse effects may not be risk-free. Like any other medical treatment, its potentially beneficial pathogen-repellant activity (which remains to be proven or refuted) may carry a tradeoff risk of adversely impacting the rate and extent of indigenous microbiome recolonization and reversion of the host gut transcriptome toward naive configuration. In contrast, new strategies, such as aFMT or person-specific microbial consortia (the latter not tested in this study), may harness individualized microbiome uniqueness in optimizing microbial colonization without adversely impacting indigenous microbiome reconstitution. Such new individualized interventions may enable achieving a more sustained live bacterial treatment efficacy upon antibiotic treatment or in a variety of other microbiome-associated medical conditions.

STAR★METHODS

Detailed methods are provided in the online version of this paper and include the following:

- KEY RESOURCES TABLE
- CONTACT FOR REAGENT AND RESOURCE SHARING

- **EXPERIMENTAL MODEL AND SUBJECT DETAILS**
 - Clinical trial
 - Exclusion and inclusion criteria (human cohorts)
 - Human Study Design
- **METHOD DETAILS**
 - Drugs and biological preparations
 - Gut microbiome sampling
 - Nucleic acid extraction
 - Nucleic acid processing and library preparation
- **QUANTIFICATION AND STATISTICAL ANALYSIS**
- **DATA AND SOFTWARE AVAILABILITY**

SUPPLEMENTAL INFORMATION

Supplemental Information includes seven figures and six tables and can be found with this article online at <https://doi.org/10.1016/j.cell.2018.08.047>.

ACKNOWLEDGMENTS

We thank the members of the Elinav and Segal laboratories for discussions and apologize to authors whose work was not included due to space constraints. We thank Refael Kohen from the Weizmann Institute of Science bioinformatics unit, Nadin Jbara from the Elinav lab, and Pierre Bost from the Amit lab for their help with DNA/RNA sequencing analysis. We thank Carmit Bar-Natan for dedicated animal husbandry. N.Z. is supported by the Gilead Sciences International Research Scholars Program in Liver Disease. J.S. is the recipient of the Strauss Institute research fellowship. E.S. is supported by the Crown Human Genome Center, the Else Kroener Fresenius Foundation, Donald L. Schwarz (Sherman Oaks, CA), Jack N. Halpern (New York, NY), Leesa Steinberg (Canada), and grants funded by the European Research Council and the Israel Science Foundation. E.E. is supported by Y. and R. Ungar, the Abisch Frenkel Foundation for the Promotion of Life Sciences, the Gurwin Family Fund for Scientific Research, the Leona M. and Harry B. Helmsley Charitable Trust, the Crown Endowment Fund for Immunological Research, the estate of J. Gitlitz, the estate of L. Hershkovich, the Benoziyo Endowment Fund for the Advancement of Science, the Adelis Foundation, J.L. and V. Schwartz, A. and G. Markovitz, A. and C. Adelson, the French National Center for Scientific Research (CNRS), D.L. Schwarz, the V.R. Schwartz Research Fellow Chair, L. Steinberg, J.N. Halpern, A. Edelheit, grants funded by the European Research Council, a Marie Curie Integration grant, the German-Israeli Foundation for Scientific Research and Development, the Israel Science Foundation, the Minerva Foundation, the Rising Tide Foundation, the Helmholtz Foundation, and the European Foundation for the Study of Diabetes. E.E. is a senior fellow of the Canadian Institute of Advanced Research (CIFAR) and an international scholar of the Bill and Melinda Gates Foundation and Howard Hughes Medical Institute (HHMI).

AUTHOR CONTRIBUTIONS

J.S., N.Z., G.Z.-S., and U.M. designed, performed, and interpreted the experiments; wrote the manuscript; and equally contributed to the study. M.D.-B., S.B., S.F., H.S., and M.P.-F. performed and assisted in experiments and sample processing. E.K., M.H., Y.C., D.Z., T.K., and I.S. performed computational analyses. A.E.M and S.I. assisted with RNA sequencing. M.Z., D.R.-L., R.B.-Z.B., N.M., and O.S assisted with patient allocation, follow-up, and procedures. A.H. oversaw animal experimentation. Z.H., E.S., and E.E. conceived the study, supervised the participants, interpreted the experiments, and wrote the manuscript.

DECLARATION OF INTERESTS

The authors declare no competing interests. Results of this work have been submitted as a patent proposal.

Received: November 13, 2017

Revised: June 5, 2018

Accepted: August 20, 2018

Published: September 6, 2018

SUPPORTING CITATIONS

The following references appear in the Supplemental Information: Furet et al. (2004), Haarman and Knol (2005), Herbel et al. (2013), Ruggirello et al. (2014), and Schwendimann et al. (2015).

REFERENCES

- Adiconis, X., Borges-Rivera, D., Satija, R., DeLuca, D.S., Busby, M.A., Berlin, A.M., Sivachenko, A., Thompson, D.A., Wysoker, A., Fennell, T., et al. (2013). Comparative analysis of RNA sequencing methods for degraded or low-input samples. *Nat. Methods* 10, 623–629.
- Allen, S.J., Wareham, K., Wang, D., Bradley, C., Hutchings, H., Harris, W., Dhar, A., Brown, H., Foden, A., Gravenor, M.B., and Mack, D. (2013). Lactobacilli and bifidobacteria in the prevention of antibiotic-associated diarrhoea and *Clostridium difficile* diarrhoea in older inpatients (PLACIDE): a randomised, double-blind, placebo-controlled, multicentre trial. *Lancet* 382, 1249–1257.
- Arvonen, M., Virta, L.J., Pokka, T., Kröger, L., and Väähäsalto, P. (2015). Repeated exposure to antibiotics in infancy: a predisposing factor for juvenile idiopathic arthritis or a sign of this group's greater susceptibility to infections? *J. Rheumatol.* 42, 521–526.
- Bafeta, A., Koh, M., Riveros, C., and Ravaud, P. (2018). Harms Reporting in Randomized Controlled Trials of Interventions Aimed at Modifying Microbiota: A Systematic Review. *Ann. Intern. Med.* Published online July 17, 2018. <https://doi.org/10.7326/M18-0343>.
- Bartlett, J.G. (2002). Clinical practice. Antibiotic-associated diarrhea. *N. Engl. J. Med.* 346, 334–339.
- Bolger, A.M., Lohse, M., and Usadel, B. (2014). Trimmomatic: a flexible trimmer for Illumina sequence data. *Bioinformatics* 30, 2114–2120.
- Caballero, S., Kim, S., Carter, R.A., Leiner, I.M., Sušac, B., Miller, L., Kim, G.J., Ling, L., and Pamer, E.G. (2017). Cooperating commensals Restore Colonization Resistance to Vancomycin-Resistant *Enterococcus faecium*. *Cell Host Microbe* 21, 592–602.
- Caporaso, J.G., Kuczynski, J., Stombaugh, J., Bittinger, K., Bushman, F.D., Costello, E.K., Fierer, N., Peña, A.G., Goodrich, J.K., Gordon, J.I., et al. (2010). QIIME allows analysis of high-throughput community sequencing data. *Nat. Methods* 7, 335–336.
- Cotter, P.D., Ross, R.P., and Hill, C. (2013). Bacteriocins - a viable alternative to antibiotics? *Nat. Rev. Microbiol.* 11, 95–105.
- Dethlefsen, L., and Relman, D.A. (2011). Incomplete recovery and individualized responses of the human distal gut microbiota to repeated antibiotic perturbation. *Proc. Natl. Acad. Sci. USA* 108 (Suppl 1), 4554–4561.
- Dethlefsen, L., Huse, S., Sogin, M.L., and Relman, D.A. (2008). The pervasive effects of an antibiotic on the human gut microbiota, as revealed by deep 16S rRNA sequencing. *PLoS Biol.* 6, e280.
- Dobin, A., Davis, C.A., Schlesinger, F., Drenkow, J., Zaleski, C., Jha, S., Batut, P., Chaisson, M., and Gingeras, T.R. (2013). STAR: ultrafast universal RNA-seq aligner. *Bioinformatics* 29, 15–21.
- Eden, E., Navon, R., Steinfeld, I., Lipson, D., and Yakhini, Z. (2009). GOriila: a tool for discovery and visualization of enriched GO terms in ranked gene lists. *BMC Bioinformatics* 10, 48.
- Ekmekciu, I., von Klitzing, E., Fiebiger, U., Neumann, C., Bacher, P., Scheffold, A., Bereswill, S., and Heimesaat, M.M. (2017). The Probiotic Compound VSL#3 Modulates Mucosal, Peripheral, and Systemic Immunity Following Murine Broad-Spectrum Antibiotic Treatment. *Front. Cell. Infect. Microbiol.* 7, 167.
- Ferrer, M., Martins dos Santos, V.A., Ott, S.J., and Moya, A. (2014). Gut microbiota disturbance during antibiotic therapy: a multi-omic approach. *Gut Microbes* 5, 64–70.

- Franker, C.K., Herbert, C.A., and Ueda, S. (1977). Bacteriocin from *Actinomyces odontolyticus* with temperature-dependent killing properties. *Antimicrob. Agents Chemother.* 12, 410–417.
- Franz, C.M., van Belkum, M.J., Holzapfel, W.H., Abriouel, H., and Gálvez, A. (2007). Diversity of enterococcal bacteriocins and their grouping in a new classification scheme. *FEMS Microbiol. Rev.* 31, 293–310.
- Furet, J.-P., Quénée, P., and Taitieze, P. (2004). Molecular quantification of lactic acid bacteria in fermented milk products using real-time quantitative PCR. *Int. J. Food Microbiol.* 97, 197–207.
- Gossens, D.A., Jonkers, D.M., Russel, M.G., Stobberingh, E.E., and Stockbrügger, R.W. (2006). The effect of a probiotic drink with *Lactobacillus plantarum* 299v on the bacterial composition in faeces and mucosal biopsies of rectum and ascending colon. *Aliment. Pharmacol. Ther.* 23, 255–263.
- Grazul, H., Kanda, L.L., and Gondek, D. (2016). Impact of probiotic supplements on microbiome diversity following antibiotic treatment of mice. *Gut Microbes* 7, 101–114.
- Haarman, M., and Knol, J. (2005). Quantitative real-time PCR assays to identify and quantify fecal *Bifidobacterium* species in infants receiving a prebiotic infant formula. *Appl. Environ. Microbiol.* 71, 2318–2324.
- Hempel, S., Newberry, S.J., Maher, A.R., Wang, Z., Miles, J.N., Shanman, R., Johnsen, B., and Shekelle, P.G. (2012). Probiotics for the prevention and treatment of antibiotic-associated diarrhea: a systematic review and meta-analysis. *JAMA* 307, 1959–1969.
- Herbel, S.R., Lauzat, B., von Nickisch-Rosenegk, M., Kuhn, M., Murugaiyan, J., Wieler, L.H., and Guenther, S. (2013). Species-specific quantification of probiotic lactobacilli in yoghurt by quantitative real-time PCR. *J. Appl. Microbiol.* 115, 1402–1410.
- Hoskin-Parr, L., Teyhan, A., Blocker, A., and Henderson, A.J. (2013). Antibiotic exposure in the first two years of life and development of asthma and other allergic diseases by 7.5 yr: a dose-dependent relationship. *Pediatr. Allergy Immunol.* 24, 762–771.
- Huber, J.A., Mark Welch, D.B., Morrison, H.G., Huse, S.M., Neal, P.R., Butterfield, D.A., and Sogin, M.L. (2007). Microbial population structures in the deep marine biosphere. *Science* 318, 97–100.
- Hyatt, D., Chen, G.L., Locascio, P.F., Land, M.L., Larimer, F.W., and Hauser, L.J. (2010). Prodigal: prokaryotic gene recognition and translation initiation site identification. *BMC Bioinformatics* 11, 119.
- Jernberg, C., Löfmark, S., Edlund, C., and Jansson, J.K. (2007). Long-term ecological impacts of antibiotic administration on the human intestinal microbiota. *ISME J.* 1, 56–66.
- Kanehisa, M., and Goto, S. (2000). KEGG: kyoto encyclopedia of genes and genomes. *Nucleic Acids Res.* 28, 27–30.
- Klarin, B., Johansson, M.L., Molin, G., Larsson, A., and Jeppsson, B. (2005). Adhesion of the probiotic bacterium *Lactobacillus plantarum* 299v onto the gut mucosa in critically ill patients: a randomised open trial. *Crit. Care* 9, R285–R293.
- Kootte, R.S., Levin, E., Salojärvi, J., Smits, L.P., Hartstra, A.V., Udayappan, S.D., Hermes, G., Bouter, K.E., Koopen, A.M., Holst, J.J., et al. (2017). Improvement of Insulin Sensitivity after Lean Donor Feces in Metabolic Syndrome Is Driven by Baseline Intestinal Microbiota Composition. *Cell Metab* 26, 611–619.
- Köster, J., and Rahmann, S. (2012). Snakemake—a scalable bioinformatics workflow engine. *Bioinformatics* 28, 2520–2522.
- Kronman, M.P., Zaoutis, T.E., Haynes, K., Feng, R., and Coffin, S.E. (2012). Antibiotic exposure and IBD development among children: a population-based cohort study. *Pediatrics* 130, e794–e803.
- Langmead, B., and Salzberg, S.L. (2012). Fast gapped-read alignment with Bowtie 2. *Nat. Methods* 9, 357–359.
- Lankelma, J.M., Cranendonk, D.R., Belzer, C., de Vos, A.F., de Vos, W.M., van der Poll, T., and Wiersinga, W.J. (2017). Antibiotic-induced gut microbiota disruption during human endotoxemia: a randomised controlled study. *Gut* 66, 1623–1630.
- Lichtman, J.S., Ferreyra, J.A., Ng, K.M., Smits, S.A., Sonnenburg, J.L., and Elias, J.E. (2016). Host-Microbiota Interactions in the Pathogenesis of Antibiotic-Associated Diseases. *Cell Rep.* 14, 1049–1061.
- Love, M.I., Huber, W., and Anders, S. (2014). Moderated estimation of fold change and dispersion for RNA-seq data with DESeq2. *Genome Biol.* 15, 550.
- Maldonado-Gómez, M.X., Martínez, I., Bottacini, F., O'Callaghan, A., Ventura, M., van Sinderen, D., Hillmann, B., Vangay, P., Knights, D., Hutkins, R.W., and Walter, J. (2016). Stable Engraftment of *Bifidobacterium longum* AH1206 in the Human Gut Depends on Individualized Features of the Resident Microbiome. *Cell Host Microbe* 20, 515–526.
- Manor, O., and Borenstein, E. (2017). Revised computational metagenomic processing uncovers hidden and biologically meaningful functional variation in the human microbiome. *Microbiome* 5, 19.
- Martin, M. (2011). Cutadapt removes adapter sequences from high-throughput sequencing reads. *EMBnet* 17, 10–12.
- McFarland, L.V. (1998). Epidemiology, risk factors and treatments for antibiotic-associated diarrhea. *Dig. Dis.* 16, 292–307.
- McFarland, L.V. (2014). Use of probiotics to correct dysbiosis of normal microbiota following disease or disruptive events: a systematic review. *BMJ Open* 4, e005047.
- Olek, A., Woynarowski, M., Ahrén, I.L., Kierkuś, J., Socha, P., Larsson, N., and Önning, G. (2017). Efficacy and Safety of *Lactobacillus plantarum* DSM 9843 (LP299V) in the Prevention of Antibiotic-Associated Gastrointestinal Symptoms in Children—Randomized, Double-Blind, Placebo-Controlled Study. *J. Pediatr.* 186, 82–86.
- Peng, Y., Leung, H.C., Yiu, S.-M., and Chin, F.Y. (2012). IDBA-UD: a de novo assembler for single-cell and metagenomic sequencing data with highly uneven depth. *Bioinformatics* 28, 1420–1428.
- Qin, J., Li, R., Raes, J., Arumugam, M., Burgdorf, K.S., Manichanh, C., Nielsen, T., Pons, N., Levenez, F., Yamada, T., et al. (2010). A human gut microbial gene catalogue established by metagenomic sequencing. *Nature* 464, 59–65.
- Risnes, K.R., Belanger, K., Murk, W., and Bracken, M.B. (2011). Antibiotic exposure by 6 months and asthma and allergy at 6 years: Findings in a cohort of 1,401 US children. *Am. J. Epidemiol.* 173, 310–318.
- Ruggirello, M., Dolci, P., and Cocolin, L. (2014). Detection and viability of *Lactococcus lactis* throughout cheese ripening. *PLoS ONE* 9, e114280.
- Schwendimann, L., Kauf, P., Fieseler, L., Gantenbein-Demarchi, C., and Miescher Schwenninger, S. (2015). Development of a quantitative PCR assay for rapid detection of *Lactobacillus plantarum* and *Lactobacillus fermentum* in cocoa bean fermentation. *J. Microbiol. Methods* 115, 94–99.
- Shao, X., Ding, X., Wang, B., Li, L., An, X., Yao, Q., Song, R., and Zhang, J.A. (2017). Antibiotic Exposure in Early Life Increases Risk of Childhood Obesity: A Systematic Review and Meta-Analysis. *Front. Endocrinol. (Lausanne)* 8, 170.
- Sharon, I., Morowitz, M.J., Thomas, B.C., Costello, E.K., Relman, D.A., and Banfield, J.F. (2013). Time series community genomics analysis reveals rapid shifts in bacterial species, strains, and phage during infant gut colonization. *Genome Res.* 23, 111–120.
- Smith, M., Kassam, Z., Edelstein, C., Burgess, J., and Alm, E. (2014). Open-Biome remains open to serve the medical community. *Nat. Biotechnol.* 32, 867.
- Strimmer, K. (2008). A unified approach to false discovery rate estimation. *BMC Bioinformatics* 9, 303.
- Suez, J., Korem, T., Zeevi, D., Zilberman-Schapira, G., Thaiss, C.A., Maza, O., Israeli, D., Zmora, N., Gilad, S., Weinberger, A., et al. (2014). Artificial sweeteners induce glucose intolerance by altering the gut microbiota. *Nature* 514, 181–186.
- Terveer, E.M., van Beurden, Y.H., Goorhuis, A., Seegers, J.F.M.L., Bauer, M.P., van Nood, E., Dijkgraaf, M.G.W., Mulder, C.J.J., Vandebroucke-Grauls, C.M.J.E., Verspaget, H.W., et al. (2017). How to: Establish and run a stool bank. *Clin. Microbiol. Infect.* 23, 924–930.
- Truong, D.T., Franzosa, E.A., Tickle, T.L., Scholz, M., Weingart, G., Pasolli, E., Tett, A., Huttenhower, C., and Segata, N. (2015). MetaPhiAn2 for enhanced metagenomic taxonomic profiling. *Nat. Methods* 12, 902–903.

- Van Boekel, T.P., Gandra, S., Ashok, A., Caudron, Q., Grenfell, B.T., Levin, S.A., and Laxminarayan, R. (2014). Global antibiotic consumption 2000 to 2010: an analysis of national pharmaceutical sales data. *Lancet Infect. Dis.* 14, 742–750.
- Vangay, P., Ward, T., Gerber, J.S., and Knights, D. (2015). Antibiotics, pediatric dysbiosis, and disease. *Cell Host Microbe* 17, 553–564.
- Virta, L., Auvinen, A., Helenius, H., Huovinen, P., and Kolho, K.L. (2012). Association of repeated exposure to antibiotics with the development of pediatric Crohn's disease—a nationwide, register-based finnish case-control study. *Am. J. Epidemiol.* 175, 775–784.
- Wiström, J., Norrby, S.R., Myhre, E.B., Eriksson, S., Granström, G., Lagergren, L., Englund, G., Nord, C.E., and Svenungsson, B. (2001). Frequency of antibiotic-associated diarrhoea in 2462 antibiotic-treated hospitalized patients: a prospective study. *J. Antimicrob. Chemother.* 47, 43–50.
- Yatsunenko, T., Rey, F.E., Manary, M.J., Trehan, I., Dominguez-Bello, M.G., Contreras, M., Magris, M., Hidalgo, G., Baldassano, R.N., Anokhin, A.P., et al. (2012). Human gut microbiome viewed across age and geography. *Nature* 486, 222–227.
- Zeevi, D., Korem, T., Zmora, N., Israeli, D., Rothschild, D., Weinberger, A., Ben-Yacob, O., Lador, D., Avnit-Sagi, T., Lotan-Pompan, M., et al. (2015). Personalized Nutrition by Prediction of Glycemic Responses. *Cell* 163, 1079–1094.
- Zmora, N., Zilberman-Schapira, G., Suez, J., Mor, U., Dori-Bachash, M., Bashiardes, S., Kotler, E., Zur, M., Regev-Lehavi, D., Brik, R.B.-Z., et al. (2018). Personalized Gut Mucosal Colonization Resistance to Empiric Probiotics Is Associated with Unique Host and Microbiome Features. *Cell* 174, this issue, 1388–1405.

STAR★METHODS

KEY RESOURCES TABLE

REAGENT or RESOURCE	SOURCE	IDENTIFIER
Bacterial and Virus Strains		
<i>Lactobacillus acidophilus</i>	N/A	Cat # ATCC 4356
<i>Lactobacillus rhamnosus</i>	Clinical isolate	N/A
<i>Lactobacillus casei</i>	N/A	Cat # ATCC 393
<i>Lactobacillus casei</i> subsp. <i>paracasei</i>	N/A	Cat # ATCC BAA-52
<i>Lactobacillus plantarum</i>	N/A	Cat # ATCC 8014
<i>Bifidobacterium longum</i> subsp. <i>infantis</i>	N/A	Cat # ATCC 15697
<i>Bifidobacterium bifidum</i>	N/A	Cat # ATCC 29521
<i>Bifidobacterium breve</i>	N/A	Cat # ATCC 15700
<i>Bifidobacterium longum</i> subsp. <i>longum</i>	N/A	Cat # ATCC 15707
<i>Lactococcus lactis</i>	Isolated from Bio 25 Supherb	N/A
<i>Streotococcus thermophilus</i>	N/A	Cat # ATCC BAA-491
Chemicals, Peptides, and Recombinant Proteins		
Bio 25 Supherb	Supherb, Nazareth Ilit, Israel	N/A
Critical Commercial Assays		
NextSeq 500/550 High Output v2 kit (150 cycles) for Metagenome shotgun sequencing	illumina	Cat# FC-404-2002
NextSeq 500/550 High Output v2 kit (75 cycles) for RNA-Seq	illumina	Cat# FC-404-2005
MiSeq Reagent Kit v2 (500-cycles)	illumina	Cat# MS-102-2003
RNeasy mini kit	QIAGEN	Cat# 74104
DNeasy PowerLyzer PowerSoil Kit	QIAGEN	Cat# 12855-100
NEBNext Ultra Directional RNA Library Prep Kit for Illumina	New England Biolabs	Cat# E7420S
NEBNext Multiplex Oligos for Illumina	New England Biolabs	Cat# E7600S
Experimental Models: Organisms/Strains		
C57BL/6JOlaHsd males 8-9 weeks of age	Envigo, Israel	N/A
Germ-free Swiss-Webster males 8-9 weeks of age	Weizmann institute of Science	N/A
Oligonucleotides		
Miseq Illumina sequencing primer	N/A	N/A
Read 1 - TATGGTAATTGTGTGCCAGCMGCCGCGTAA		
Miseq Illumina sequencing primer	N/A	N/A
Read 2 - AGTCAGTCAGCCGGACTACHVGGGTWTCTAAT		
Miseq Illumina sequencing primer	N/A	N/A
Index primer - ATTAGAWACCCBDGTAGTCCGGCTGACTGACT		
16S qPCR 111-967F-PP:CNACGCGAAGAACCTTANC	(Huber et al., 2007)	N/A
16S qPCR 112-967F-UC3:ATACCGCGARGAACCTTACC	(Huber et al., 2007)	N/A
16S qPCR 113-967F-AQ:CTAACCGANGAACCTYACC	(Huber et al., 2007)	N/A
16S qPCR 114-967F-S:CAACGCGMARAACCTTACC	(Huber et al., 2007)	N/A
16S qPCR 115-1046R-S:CGACRRCCATGCANACCT	(Huber et al., 2007)	N/A
Deposited Data		
Sequence data	European Nucleotide Archive	ENA: PRJEB28097
Software and Algorithms		
QIIME 1.9.1	Caporaso et al., 2010	N/A
Trimmomatic	Bolger et al., 2014	N/A

(Continued on next page)

Continued

REAGENT or RESOURCE	SOURCE	IDENTIFIER
MetaPhlAn2	Truong et al., 2015	N/A
Bowtie2	Langmead and Salzberg, 2012	N/A
EMPA NADA	Manor and Borenstein, 2017	N/A
GOrilla (Gene Ontology enRICHment anaLysis and visuaLizAtion tool)	Eden et al., 2009	N/A

CONTACT FOR REAGENT AND RESOURCE SHARING

Further information and requests for resources and reagents may be directed to and will be fulfilled by the Lead Contact, Eran Elinav (eran.elinav@weizmann.ac.il).

EXPERIMENTAL MODEL AND SUBJECT DETAILS**Clinical trial**

The human MUSPIC trials were approved by the Tel Aviv Sourasky Medical Center Institutional Review Board (IRB approval numbers TLV-0553-12, TLV-0658-12 and TLV-0196-13) and Weizmann Institute of Science Bioethics and Embryonic Stem Cell Research oversight committee (IRB approval numbers 421-1, 430-1 and 444-1), and were reported to <https://clinicaltrials.gov/> (Identifiers: NCT03218579 and NCT01922830). Written informed consent was obtained from all subjects.

Exclusion and inclusion criteria (human cohorts)

All subjects fulfilled the following inclusion criteria: males and females, aged 18–70, who are currently not following any diet regimen or dietitian consultation and are able to provide informed consent. Exclusion criteria included: (i) pregnancy or fertility treatments; (ii) usage of antibiotics or antifungals within three months prior to participation; (iii) consumption of probiotics in any form within one month prior to participation, (iv) chronically active inflammatory or neoplastic disease in the three years prior to enrollment; (v) chronic gastrointestinal disorder, including inflammatory bowel disease and celiac disease; (vi) active neuropsychiatric disorder; (vii) myocardial infarction or cerebrovascular accident in the six months prior to participation; (viii) coagulation disorders; (ix) chronic immunosuppressive medication usage; (x) pre-diagnosed type I or type II diabetes mellitus or treatment with anti-diabetic medication. Fulfillment of inclusion and exclusion criteria was validated by medical doctors.

Human Study Design

Forty-six healthy volunteers were recruited for this study between the years 2014 and 2018 (see Table S1). Upon enrollment, participants were required to fill up medical, lifestyle and food frequency questionnaires, which were reviewed by medical doctors before the acceptance to participate in the study. Two cohorts were recruited, a naive cohort ($n = 25$) and an antibiotics-treated cohort ($n = 21$), subdivided into three interventions of probiotics ($n = 8$), autologous fecal microbiome transplantation (aFMT, $n = 6$) and spontaneous reconstitution ($n = 7$). For the antibiotics-treated cohort, the study design consisted of four phases, baseline (7 days), antibiotics (7 days), intervention (28 days) and follow-up (28 days). During the 4-week intervention phase (days 1 through 28), participants from the probiotics arm were instructed to consume a commercial probiotic supplement (Bio-25) bi-daily; participants from the aFMT arm received an intrajejunal infusion of 150 ml of processed and liquefied stool (on day 0), which had been obtained from the participant prior to the antibiotics therapy; and participants from the spontaneous reconstitution group did not undergo any treatment. Stool samples were collected daily during the baseline and antibiotics phases, daily during the first week of intervention and then weekly throughout the rest of the intervention, bi-monthly and monthly during the follow-up phase. Participants in the antibiotics cohort underwent two endoscopic examinations, one at the end of the antibiotics phase (day 0) and another three weeks through the intervention phase (day 21). Participants in the naive cohort underwent a single endoscopic examination, of whom ten collected daily stool samples on the seven days prior to the endoscopy.

All 46 subjects completed the trial as planned and there were no dropouts or withdrawals. In this trial, 10 minor adverse events were reported and fully resolved. All participants received payment for their participation in the study upon discharge from their last endoscopic session.

METHOD DETAILS**Drugs and biological preparations****Antibiotics**

During the antibiotics phase participants were required to consume oral ciprofloxacin 500 mg (Ciprofloxacin, Dexcel Pharma) bi-daily and oral metronidazole 500 mg (Flagyl, Sanofi) tri-daily for a period of 7 days.

Probiotics

During the probiotics phase participants consumed Supherb Bio-25 bi-daily, which is described by the manufacturer to contain at least 25 billion active bacteria of the following species: *B. bifidum*, *L. rhamnosus*, *L. lactis*, *L. casei* subsp. *casei*, *B. breve*, *S. thermophilus*, *B. longum* subsp. *longum*, *L. casei* subsp. *paracasei*, *L. plantarum* and *B. longum* subsp. *infantis*. The pills underwent double coating to ensure their survival under stomach acidity and their proliferation in the intestines. Validation of the aforementioned species quantity and viability was performed as part of the study (Zmora et al., 2018).

Autologous fecal microbiome transplantation

Participants assigned to the aFMT study arm were requested to attend the bacteriotherapy unit of the Tel Aviv Sourasky Medical Center and deposit a fresh stool sample of at least 350 gr. The sample promptly underwent embedding in glycerol, homogenization, filtering and was transferred to storage at -80°C. The sample was thawed 30 min prior to the endoscopic procedure and placed in syringes. A volume of 150 ml of the preparation was given as an intrajejunal infusion at the end of the first (post-antibiotics) endoscopic examination. The average fecal content was 70.02 ± 22.28 gr per 150 ml suspension.

Gut microbiome sampling

Stool sampling

Participants were requested to self-sample their stool on pre-determined intervals (as previously described) using a swab following detailed printed instructions. Collected samples were immediately stored in a home freezer (-20°C) for no more than 7 days and transferred in a provided cooler to our facilities, where they were stored at -80°C.

Endoscopic examination

Forty-eight hours prior to the endoscopic examination, participants were asked to follow a pre-endoscopy diet. 20 hours prior to the examination diet was restricted to clear liquids. All participants underwent a sodium picosulfate (Pico Salax)-based bowel preparation. Participants were equipped with two fleet enemas, which they were advised to use in case of unclear stools. The examination was performed using a Pentax 90i endoscope (Pentax Medical) under light sedation with propofol-midazolam.

Luminal content was aspirated from the stomach, duodenum, jejunum, terminal ileum, cecum and descending colon into 15 ml tubes by the endoscope suction apparatus and placed immediately in liquid nitrogen. Brush cytology (US Endoscopy) was used to scrape the gut lining to obtain mucosal content from the gastric fundus, gastric antrum, duodenal bulb, jejunum, terminal ileum, cecum, ascending colon, transverse colon, descending colon, sigmoid colon and rectum. Brushes were placed in screw cap micro tubes and were snap-frozen in liquid nitrogen. Biopsies from the gut epithelium were obtained from the stomach, duodenum, jejunum, terminal ileum, cecum, and descending colon and were snap-frozen in liquid nitrogen. By the end of each session, all samples were transferred to Weizmann Institute of Science and stored in -80°C.

Mouse study design

Eight-week old male C57BL/6 mice (average initial weight 20 gr) were purchased from Harlan Envigo and allowed to acclimatize to the animal facility environment for two weeks prior to the experiments. In all experiments, age- and gender-matched mice were used. All mice were kept at a strict 24 hr light-dark cycle, with lights on from 6am to 6pm. Every experimental group consisted of two cages per group to control for cage effect (n = 5 per cage). For antibiotic treatment, mice were given a combination of ciprofloxacin (0.2 g/l, Sigma-Aldrich) and metronidazole (1 g/l, LKT laboratories) in their drinking water for two weeks as previously described (Suez et al., 2014). For probiotics supplementation, a single pill (Supherb Bio-25) was dissolved in 10 ml of sterile PBS and immediately fed to mice by oral gavage during the dark phase (4×10^9 CFU kg⁻¹ day⁻¹). For aFMT, fecal pellets were collected prior to antibiotics administration and snap-frozen in liquid nitrogen; during the day of aFMT, the pellets from each mouse were separately resuspended in sterile PBS under anaerobic conditions (Coy Laboratory Products, 75% N₂, 20% CO₂, 5% H₂), vortexed for three minutes and allowed to settle by gravity for 2 min. Samples were immediately transferred to the animal facility in Hungate anaerobic culture tubes and the supernatant was administered to the mice by oral gavage. Stool was collected on pre-determined days at the beginning of the dark phase, and immediately snap-frozen and transferred for storage at -80°C until further processing. During each time point, each group was handled by a different researcher in one biological hood to minimize cross-contamination. Upon the termination of experiments, mice were sacrificed by CO₂ asphyxiation, and laparotomy was performed by employing a vertical midline incision. After the exposure and removal of the digestive tract, it was dissected into eight parts: the stomach; beginning at the pylorus, the proximal four cm of the small intestine was collected as the duodenum; the following third of the small intestine was collected as the proximal and distal jejunum; the ileum was harvested as the distal third of the small intestine; the cecum; lastly, the colon was divided into its proximal and distal parts. For each section, the content within the cavity was extracted and collected for luminal microbiome isolation, and the remaining tissue was rinsed three times with sterile PBS and collected for mucosal microbiome isolation. A total of 710 fecal samples, 680 luminal and 680 mucosal samples were analyzed. All animal studies were approved by the Weizmann Institute of Science Institutional Animal Care and Use committee (IACUC), application number 29530816-2.

Bacterial cultures

Bacterial strains used in this study are listed in the [Key Resource Table](#). For culturing of bacteria from the probiotics pill, the following liquid media were used: De Man, Rogosa and Sharpe (MRS), modified reinforced clostridial (RC), M17, Brain-Heart Infusion (BHI), or chopped meat carbohydrate medium (CM). All growth media were purchased from BD. Cultures were grown under anaerobic

conditions (Coy Laboratory Products, 75% N₂, 20% CO₂, 5% H₂) in 37°C without shaking. For fecal microbiome cultures, ~200 mg of frozen human feces was vortexed in 5 ml of BHI under anaerobic conditions. 200 µl of the supernatant were transferred to fresh 5 ml of BHI for initiation of growth. Stationary phase probiotics cultures were filtered using a 0.22 µM filter and added to the fecal culture. For pure *Lactobacillus* cultures, each strain was grown in liquid MRS under anaerobic conditions.

Nucleic acid extraction

DNA purification

DNA was isolated from endoscopic samples, both luminal content and mucosal brushes, using DNeasy PowerLyzer PowerSoil Kit (QIAGEN). DNA was isolated from stool swabs using PowerMag Soil DNA Isolation Kit (QIAGEN) optimized for an automated platform.

RNA Purification

Gastrointestinal biopsies obtained from the participants were purified using RNAeasy kit (QIAGEN, 74104) according to the manufacturer's instructions. Most of the biopsies were kept in RNAlater solution (ThermoFisher, AM7020) and were snap-frozen in liquid nitrogen.

Nucleic acid processing and library preparation

qPCR Protocol for Quantification of Bacterial DNA

DNA templates were diluted to 1 ng per reaction before amplifications with the primer sets (indicated in Table S3) using the Fast Sybr Green Master Mix (ThermoFisher) in duplicates. Amplification conditions were: denaturation 95°C for three minutes, followed by 40 cycles of denaturation 95°C for 3 s; annealing 64°C for 30 s followed by meting curve. Duplicates with > 2 cycle difference were excluded from analysis. The CT value for any sample not amplified after 40 cycles was defined as 40 (threshold of detection).

16S rDNA Sequencing

For 16S amplicon pyrosequencing, PCR amplification was performed spanning the V4 region using the primers 515F/806R of the 16S rRNA gene and subsequently sequenced using 2X250 bp paired-end sequencing (Illumina MiSeq). Custom primers were added to Illumina MiSeq kit resulting in 253 bp fragment sequenced following paired end joining to a depth of 110,998 ± 66,946 reads (mean ± SD).

Read1: TATGGTAATTGTGTGCCAGCMGCCGCGTAA

Read2: AGTCAGTCAGCCGGACTACHVGGGTWTCTAAT

Index sequence primer: ATTAGAWACCCBDGTAGTCGGCTGACTGACTATTAGAA

Whole genome shotgun sequencing

100 ng of purified DNA was sheared with a Covaris E220X sonicator. Illumina compatible libraries were prepared as described (Suez et al., 2014), and sequenced on the Illumina NextSeq platform with a read length of 80bp to a depth of 6294093 ± 5732308 (stool) or 3366309 ± 4950053 (lumen and mucosa) reads (mean ± SD).

RNA-Seq

Ribosomal RNA was selectively depleted by RnaseH (New England Biolabs, M0297) according to a modified version of a published method (Adiconis et al., 2013). Specifically, a pool of 50 bp DNA oligos (25 nM, IDT, indicated in Table S4) that is complementary to murine rRNA18S and 28S, was resuspended in 75 µl of 10 mM Tris pH 8.0. Total RNA (100-1000 ng in 10 µl H₂O) were mixed with an equal amount of rRNA oligo pool, diluted to 2 µl and 3 µl 5x rRNA hybridization buffer (0.5 M Tris-HCl, 1 M NaCl, titrated with HCl to pH 7.4) was added. Samples were incubated at 95°C for 2 min, then the temperature was slowly decreased (~0.1°C/s) to 37°C. RNaseH enzyme mix (2 µl of 10 U RNaseH, 2 µL 10x RNaseH buffer, 1 µL H₂O, total 5 µl mix) was prepared 5 min before the end of the hybridization and preheated to 37°C. The enzyme mix was added to the samples when they reached 37°C and they were incubated at this temperature for 30 min. Samples were purified with 2.2x SPRI beads (Ampure XP, Beckmann Coulter) according to the manufacturers' instructions. Residual oligos were removed with DNase treatment (ThermoFisher Scientific, AM2238) by incubation with 5 µl DNase reaction mix (1 µl Trubo DNase, 2.5 µl Turbo DNase 10x buffer, 1.5 µl H₂O) that was incubated at 37°C for 30 min. Samples were again purified with 2.2x SPRI beads and suspended in 3.6 µl priming mix (0.3 µl random primers of New England Biolab, E7420, 3.3 µl H₂O). Samples were subsequently primed at 65°C for 5 min. Samples were then transferred to ice and 2 µl of the first strand mix was added (1 µl 5x first strand buffer, NEB E7420; 0.125 µl RNase inhibitor, NEB E7420; 0.25 µl ProtoScript II reverse transcriptase, NEB E7420; and 0.625 µl of 0.2 µg/ µl Actinomycin D, Sigma, A1410). The first strand synthesis and all subsequent library preparation steps were performed using NEBNext Ultra Directional RNA Library Prep Kit for Illumina (NEB, E7420) according to the manufacturers' instructions (all reaction volumes reduced to a quarter).

16S rDNA analysis

The 2X250 bp reads were processed using the QIIME (Caporaso et al., 2010) (Quantitative Insights Into Microbial Ecology, <http://www.qiime.org>) analysis pipeline. In brief, FASTA quality files and a mapping file indicating the barcode sequence corresponding to each sample were used as inputs. Paired reads were first assembled into longer reads based on sequence similarity, and then split to samples according to the barcodes. Sequences sharing > 97% nucleotide sequence identity in the 16S rRNA region were

binned into operational taxonomic units (97% ID OTUs). Each OTU was assigned a taxonomical classification by applying the Uclust algorithm against the Greengenes database, and an OTU table was created.

Metagenomic analysis

Data from the sequencer was converted to fastq files with bcl2fastq. Reads were then QC trimmed using Trimmomatic (Bolger et al., 2014) with parameters PE -threads 10 -phred33 -validatePairs ILLUMINACLIP:TruSeq3-PE.fa:2:30:10 LEADING:3 TRAILING:3 MINLEN:50. We used MetaPhlAn2 (Truong et al., 2015) for taxonomic analysis with the parameters: --ignore_viruses --ignore_archaea --ignore_eukaryotes.

Host sequences were removed by aligning the reads against human genome reference hg19 using bowtie2 (Langmead and Salzberg, 2012) with the parameters: -D 5 -R 1 -N 0 -L 22 -i S,0,2.50. The resulting non-host reads were then mapped to the integrated gene catalog (Qin et al., 2010) using bowtie2 with parameters:--local -D 25 -R 3 -N 1 -L 19 -i S,1,0.25 -k 5 allowing to a single read to match up to five different entries.

Further filtering of the bacterial reads consisted of retaining only records with minimal base quality of 26. The resulting bacterial quality-filtered bam files were then subsampled to 1×10^5 and 5×10^5 bacterial hits for endoscopic and stool samples, respectively. An entry's score was defined by its length, divided by the gene length. Entries' scores were summarized according to KO annotations (Kanehisa and Goto, 2000). Each sample was scaled to 1M. KEGG Pathway analysis was conducted using EMPANADA (Manor and Borenstein, 2017).

Probiotics strain identification by unique genomic sequences

To evaluate the presence of the probiotic strains using metagenomics data we applied a pipeline aimed at determining whether a strain's species is present in the sample, and then whether one of the strains for the species in the sample is the probiotics strain.

Preparation step: genome recovery of probiotics strains. Genomes of the probiotic strains were reconstructed from metagenomics samples of the probiotics pills used in the study. Assembly was performed using idba-ud (Peng et al., 2012), followed by genome closing procedures that relied on connecting scaffolds using paired-end read data and mini-assembly (Sharon et al., 2013). Genomes for the most abundant strains were recovered first using part of the data. Less abundant genomes were recovered next after removing the reads for the abundant genomes from the samples and using all the remaining data. Genes and proteins were predicted for each genome using prodigal (Hyatt et al., 2010). The abundance of different strains was evaluated and the amount of data required for each genome was estimated by MetaPhlAn2 (Truong et al., 2015). Statistics for the recovered genomes and closest published strains are provided in Table S5. All genomes but *B. longum* were assembled at an estimated completeness of > 94% and contamination of < 4%. *B. longum* was probably represented by two strains, of which we were able to assemble and identify the common regions (roughly half of the genome sizes). All probiotic strains but *L. lactis* and *L. paracasei* had nearly identical published reference genomes.

Evaluating the presence of probiotics strains in metagenomics samples:

1. Removal of human reads from samples. Metagenomic reads were mapped against the human genome (GRCh38.p7, downloaded from NCBI) using bowtie2 (Langmead and Salzberg, 2012) with the parameter: --very_sensitive. All read pairs, in which one or both reads aligned to the genome, were removed from further analysis.
2. Identifying reads that potentially belong to the probiotic strains. Metagenomic reads were mapped against the recovered probiotic genomes using bowtie2 with the parameter: --very_sensitive. All mapped reads and their paired-ends were considered further in the analysis.
3. Assigning reads to probiotic genomes. All reads recovered in the previous step were aligned against a database consisting of all probiotic genomes as well as genomes downloaded from RefSeq, which belong to the orders Bifidobacteriales and Lactobacillales (maximum of 10 genomes for each species). Alignment was done using bowtie2 with the parameter: --very_sensitive. Reads that best aligned to one of the probiotic strains were assigned to the strain along with their paired-end.
4. Determining species presence in each sample. For each probiotic strain, the percent of its genes expected to be covered by at least one read was estimated as a function of the observed genome coverage. This was done through simulations, in which different numbers of reads from one of the metagenomic samples of the probiotic pill were aligned against each of the probiotic genomes. Based on these simulations we designed a function that bound 95% of the simulated samples using R functions loess.SD (package msir) and approxfun. The threshold was set to half of the resulting function value for each coverage.
5. Identifying strain-specific genes in each probiotic genome. This step was necessary for the identification of the probiotic strains in the samples (see next step) and included: downloading available genomes of other strains for the same species from NCBI's RefSeq and comparing each reference genome to the probiotic strain genome using compare-sets.pl (<https://github.com/CK7/compare-sets>) with a 96% similarity threshold. Genomes that aligned at $\geq 70\%$ of their length were labeled "similar" while genomes that aligned at $\geq 98\%$ of their size were labeled "nearly identical." Then genes of the probiotic strain were aligned against all similar/nearly identical genomes using blastn. A gene was identified as strain-specific gene if it aligned to at least one other genome at $>= 60\%$ identity, and aligned to no more than 10% of the similar (but not nearly identical) genomes. Table S6 summarizes the number of genes and strain-specific genes for each probiotic strain.

- Determining probiotic strain presence in each sample. We characterized the presence of strain genes that were expected to be covered by at least one read for each percent of all genes covered by one or more reads using simulations. Based on the simulations we designed functions that bound 95% and 99% of the simulated results using R functions loess.SD and approxfun. Assignment of probiotic strains to species was done according to the following key: 'Unknown', < 20% of all genes were covered by at least one read; 'Do not contain the probiotic strain', the fraction of strain specific genes were below the 99% function; 'Possibly contain the probiotic strain', samples in which the fraction of strain genes was between the 95% to the 99% functions; 'Contain the probiotic strain', the fraction of strain genes was above the 95% function.

RNA-seq analysis

Reads were trimmed using cutadapt (Martin, 2011) and mapped to hg38 *Homo sapiens* genome using STAR (Dobin et al., 2013) v2.4.2a (default parameters). Genes were annotated using RefSeq. Genes having a minimum of 5 reads in at least one sample were considered for further analysis. Normalization of the counts and differential expression analysis was performed using DESeq2 (Love et al., 2014) with the parameters: betaPrior = True, cooksCutoff = FALSE, independentFiltering = FALSE. Raw P values were adjusted for multiple testing using the procedure of Benjamini and Hochberg. The p-adjusted values were corrected by fdrt (Strimmer, 2008) if one of the following applies: (A) The pipeline computed the fractions of the p values in range between [0.25,1] for the following bins: [0.25,0.5], [0.5,0.75], [0.75,1], and the fractions of the p values in one of the bins is not between 0.28 to 0.38. (B) The fraction of the p values in the range [0,0.25] is lower from the fraction of the p values of the range [0.25,1] by 0.05. Pipeline was constructed using Snakemake (Köster and Rahmann, 2012).

QUANTIFICATION AND STATISTICAL ANALYSIS

The following statistical analyses were applied unless specifically stated otherwise: for 16S data, rare OTUs (< 0.1% in relative abundance) were filtered out, and samples were then rarefied to a depth of 10,000 reads. For metagenomic data, samples with < 1X10⁵ (endoscopic samples) or < 5X10⁵ (stool samples) assigned bacterial reads (after host removal) were excluded from further analysis. In the remaining samples, rare KEGG orthologous (KO) genes (< 0.1%) were removed. Beta diversity was calculated on OTUs (16S) or species (metagenomics) relative abundances using UniFrac distances or Bray-Curtis dissimilarity (R Vegan package, <https://cran.r-project.org/web/packages/vegan/index.html>), respectively. Beta diversity for KOs and functional bacterial pathways was calculated using Spearman's rank correlation coefficient. Alpha diversity was calculated on OTUs (16S) using the observed species index. For 16S data, measurements of alpha and beta diversity were calculated using QIIME tools v 1.9.1. In order to determine the effect of treatment on microbiota taxonomic composition and functional capacity repeated-measures Kruskal Wallis with Dunn's test was used. In order to compare the effect of treatment over time between two groups or more Two-Way ANOVA with Dunnett's test, or permutation tests performed by switching labels between participants (in a paired fashion when suitable), including all their assigned samples, were used. Mann-Whitney and Wilcoxon tests were used to conduct pairwise comparisons between two treatment arms or two groups of participants. Permutational multivariate ANOVA (Adonis PERMANOVA with 10,000 permutations) based on sample distances was used to test for changes in the community composition and function. To analyze qPCR data, Two way ANOVA with Sidak or Dunnett test was used. The threshold of significance was determined to be 0.05 both for p and q-values. Statistically significant findings were marked according to the following cutoffs: *, p < 0.05; **, p < 0.01; ***, p < 0.001; ****, p < 0.0001. Data were plotted with GraphPad Prism version 7.0c. Statistical details for all experiments, including sample size, the statistical test used, dispersion and precision measures and statistical significance, are specified in the result section and denoted in figure legends.

DATA AND SOFTWARE AVAILABILITY

Sequence data have been deposited in the European Nucleotide Archive under accession number ENA: PRJEB28097.

Supplemental Figures

Cell

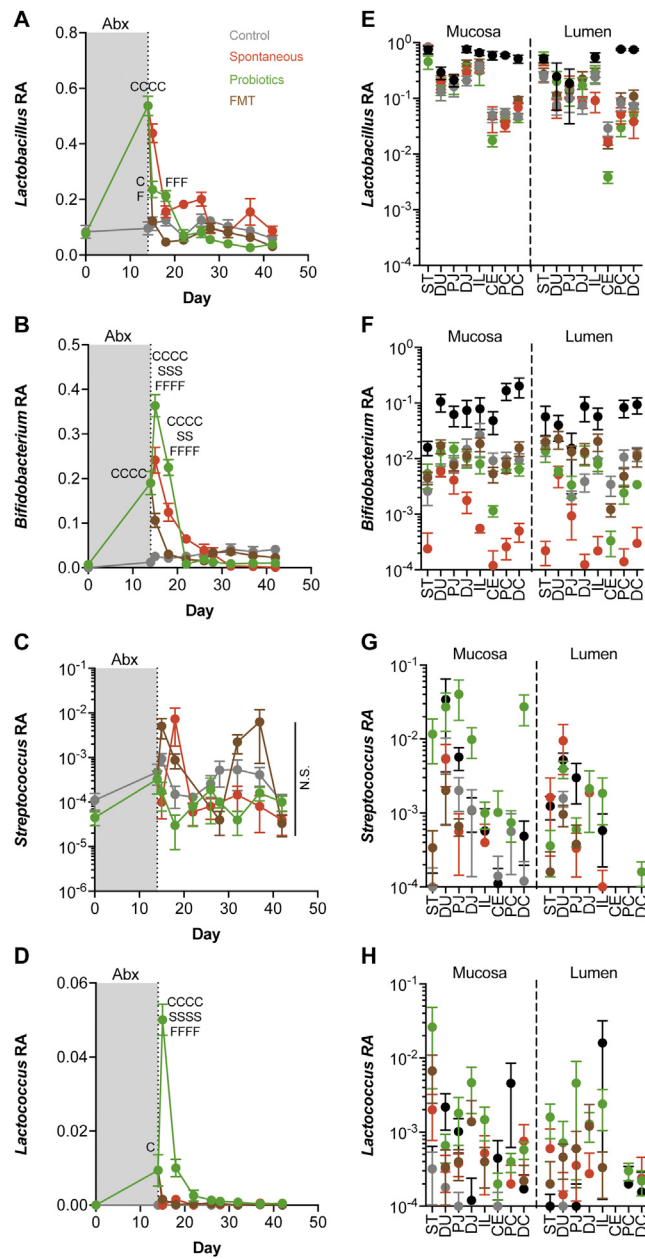


Figure S1. Kinetics of Post-Antibiotic Probiotic Colonization in the Murine Gastrointestinal Tract, Related to Figure 1

(A–H) 16S rDNA-based quantification of probiotics genera in (A–D) stool or (E–H) lumen and mucosa GI samples of male adult C57BL/6 WT mice treated with ciprofloxacin & metronidazole followed by no intervention ($n = 10$, spontaneous recovery, S), aFMT of a pre-antibiotics fecal sample (F, $n = 10$) or daily administration of probiotics (P, $n = 10$). A fourth control group was antibiotics-naïve (C, $n = 10$). In (E)–(H), a fifth group ($n = 10$), dissected immediately after antibiotics, is included in black. Portrayed are the relative abundances (RA) of (A) and (E) *Lactobacillus* (B and F) *Bifidobacterium* (C and G) *Streptococcus* (D and H) *Lactococcus*. Letters above symbols denote probiotics higher and significant versus control ("C"), aFMT ("F") or spontaneous recovery (S), repeated letters correspond to magnitude of p value according to Two-Way ANOVA & Dunnett. * $p < 0.05$; ** $p < 0.01$; *** $p < 0.001$; **** $p < 0.0001$; N.S., non-significant. Symbols represent the mean; error bars SEM.

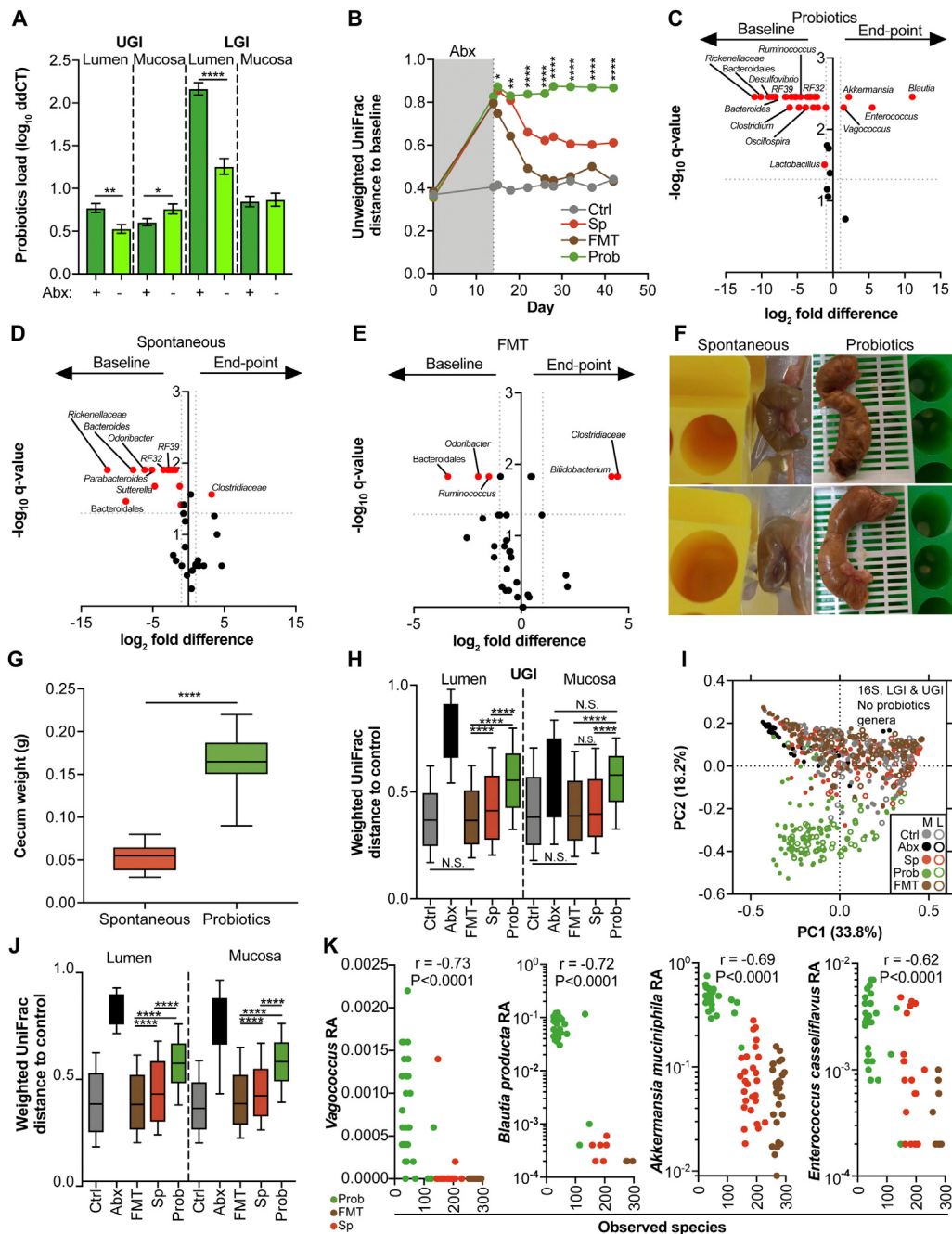


Figure S2. Probiotics Delay while aFMT Enhances the Post-Antibiotics Fecal and GI Murine Microbiome Reconstitution, Related to Figure 2
 (A) qPCR-based aggregated probiotics load in UGI and LGI tissues of antibiotics-treated (+) or naive mice (-, independent cohort described elsewhere (Zmora et al., 2018). *p < 0.05; **p < 0.01; ***p < 0.0001, Mann-Whitney.

(B) Unweighted UniFrac distances in fecal samples were recalculated after omitting the four probiotics genera (*Lactobacillus*, *Bifidobacterium*, *Lactococcus*, and *Streptococcus*) from the OTU table, followed by rarefaction to 10,000 reads and renormalizing to 1. *p < 0.05; **p < 0.01; ***p < 0.0001, Two-Way ANOVA and Dunnett between probiotics and spontaneous recovery.

(C–E) Significant differences (FDR corrected Wilcoxon rank sum test p < 0.05) in fecal microbiome following the various post-antibiotics treatments highlighted in red. (C) 28-days probiotics (D) no post-antibiotics treatment, spontaneous recovery (E) aFMT.

(F and G) Macroscopic differences in mice ceca between post-antibiotics probiotics and spontaneous recovery. Ceca were harvested 28 days post-antibiotics and probiotics supplementation or no treatment. (F) Larger ceca are observed in probiotics mice, some with a black spot. (G) Probiotics mice have heavier ceca, Mann-Whitney p < 0.0001.

(legend continued on next page)

(H) Weighted UniFrac distances to control. ***p < 0.0001; N.S., non-significant, Kruskal-Wallis & Dunn's.

(I and J) Same as (B) but in tissues, re-rarefied to 5,000 reads.

(K) Top taxa significantly anti-correlated with alpha diversity in the LGI mucosa. Samples are colored according to group. Significance and r-values according to Spearman. Symbols and horizontal lines represent the mean, error bars SEM or 10-90 percentile.

Ctrl, control; Sp, spontaneous recovery; Prob, probiotics. LGI, lower gastrointestinal tissues; UGI, upper gastrointestinal tissues. L, lumen; M, mucosa.

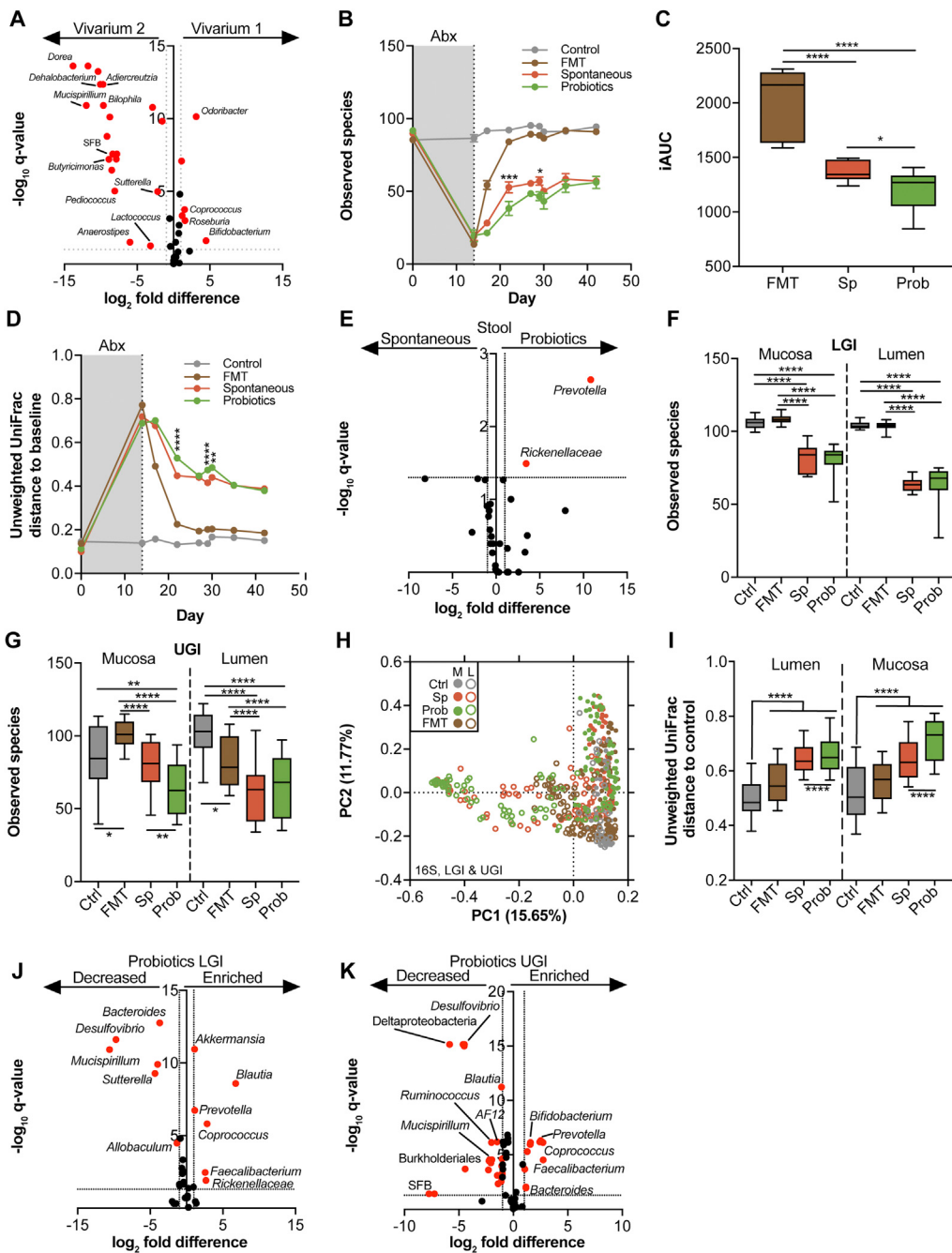


Figure S3. Validation Mouse Cohort in a Different Vivarium, Related to Figure 2

Experimental conditions detailed in Figure 2 were repeated in an independent group of mice in a different vivarium. 16S rDNA-based comparison of post ciprofloxacin and metronidazole reconstitution in probiotics treated mice ($n = 10$) compared to mice treated with aFMT ($n = 10$), mice that did not receive post-antibiotics treatment ($n = 10$), and a fourth antibiotics-naïve control group ($n = 10$).

(A) Taxa significantly different between the vivaria represented in stool samples, red circles denote an FDR-corrected Mann-Whitney $p < 0.05$.

(B) Stool alpha diversity. * $p < 0.05$; ** $p < 0.001$, Two-Way ANOVA & Tukey between spontaneous recovery and probiotics.

(C) Post-antibiotics incremental area under the alpha diversity reconstitution curve from last day of antibiotics (IACU). * $p < 0.05$; *** $p < 0.0001$, Kruskal-Wallis & Dunn's.

(D) Unweighted UniFrac distances to baseline in feces. Asterisks denote significance between probiotics and spontaneous recovery, Two-Way ANOVA & Tukey.

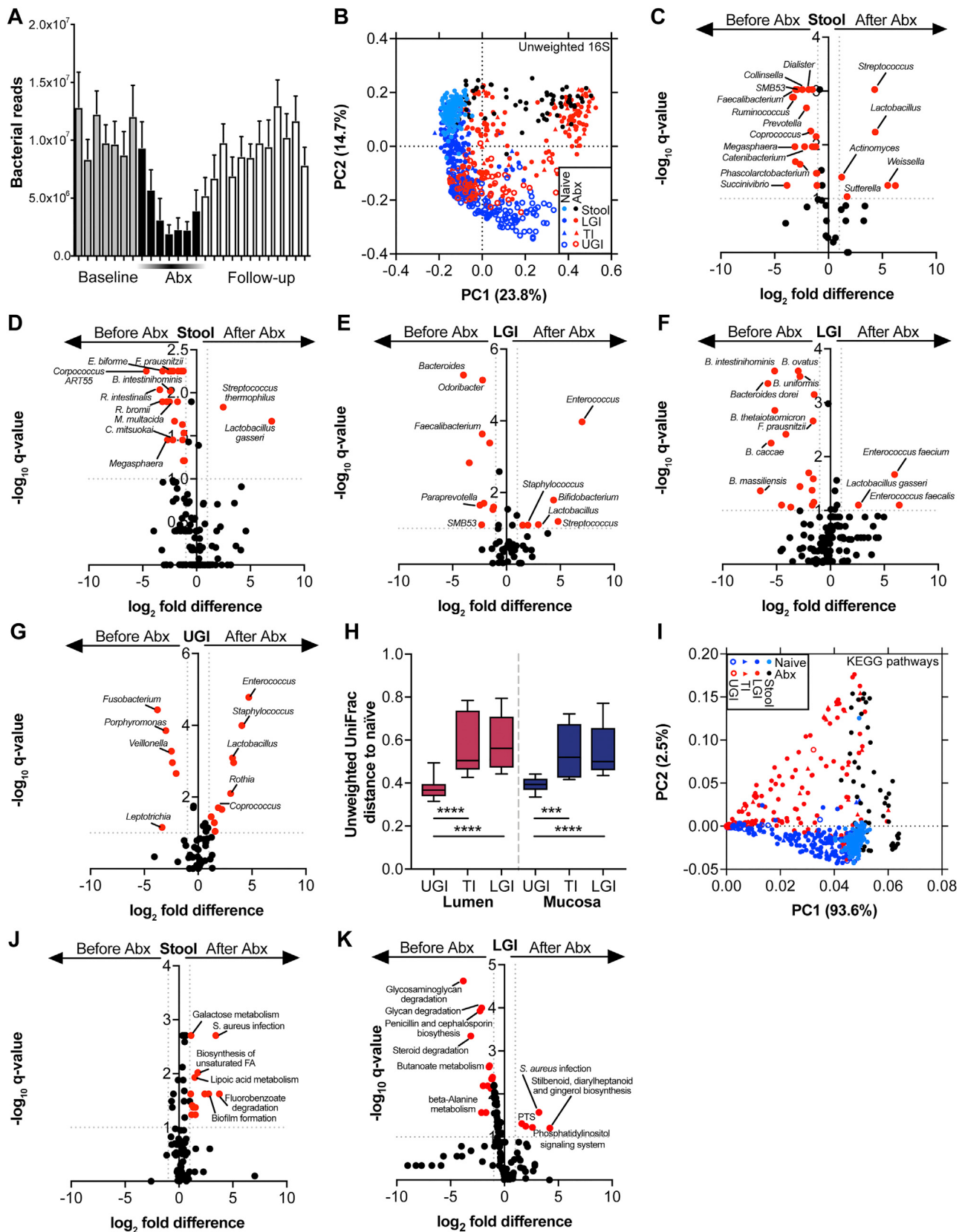
(E) Taxa significantly (FDR-corrected Mann-Whitney $p < 0.05$) over represented in stool samples after 28 days of probiotics compared to no treatment.

(F and G) Alpha diversity in tissues of the (F) LGI and (G) UGI, significance according to Kruskal-Wallis & Dunn's.

(H and I) Unweighted UniFrac distances to control in tissues. Significance is according to Kruskal-Wallis & Dunn's.

(legend continued on next page)

(J and K) Taxa significantly enriched or decreased in probiotics compared to spontaneous recovery and aFMT together in the (J) LGI or (K) UGI. Red circles have an FDR-corrected Mann-Whitney $p < 0.05$. Symbols and horizontal lines represent the mean, error bars SEM or 10-90 percentile. * $p < 0.05$; ** $p < 0.01$; *** $p < 0.001$; **** $p < 0.00001$.
Abx, antibiotics; LGI, lower gastrointestinal tissues; UGI, upper gastrointestinal tissues; L, lumen; M, mucosa. Ctrl, control; Sp, spontaneous recovery; Prob, probiotics.



(legend on next page)

Figure S4. Antibiotics-Mediated Alterations to the Human Gut Microbiome Composition and Function, Related to Figure 3

(A) Reduction in shotgun sequencing reads from stool mapped to bacteria by Bowtie2 during antibiotics.

(B) PCoA based on 16S rDNA composition post-antibiotics or in an antibiotics-naive cohort (Zmora et al., 2018).

(C and D) Genera (C) or species (D) significantly altered by antibiotics in stool samples, red circles have an FDR-corrected Wilcoxon signed-rank test $p < 0.05$. All pre-antibiotics stool samples from all participants compared to days 4–7 of antibiotics.

(E and F) Same as (C) and (D) but in the LGI mucosa.

(G) Same as (E) but in the UGI mucosa.

(H) Unweighted UniFrac distances of various GI regions to the corresponding region in a separate, antibiotics-naive cohort ($n = 19$; Zmora et al., 2018). Significance according to Kruskal-Wallis & Dunn's.

(I) Same as (B) but PCA based on KEGG pathways.

(J) Same as (C) but with KEGG pathways.

(K) Same as (J) but in the LGI mucosa. Horizontal lines represent the mean; error bars represent SEM or 10–90 percentile. * $p < 0.05$; ** $p < 0.01$; *** $p < 0.001$; **** $p < 0.0001$.

Abx, antibiotics, UGI, upper gastrointestinal, LGI, lower gastrointestinal, TI, terminal ileum.

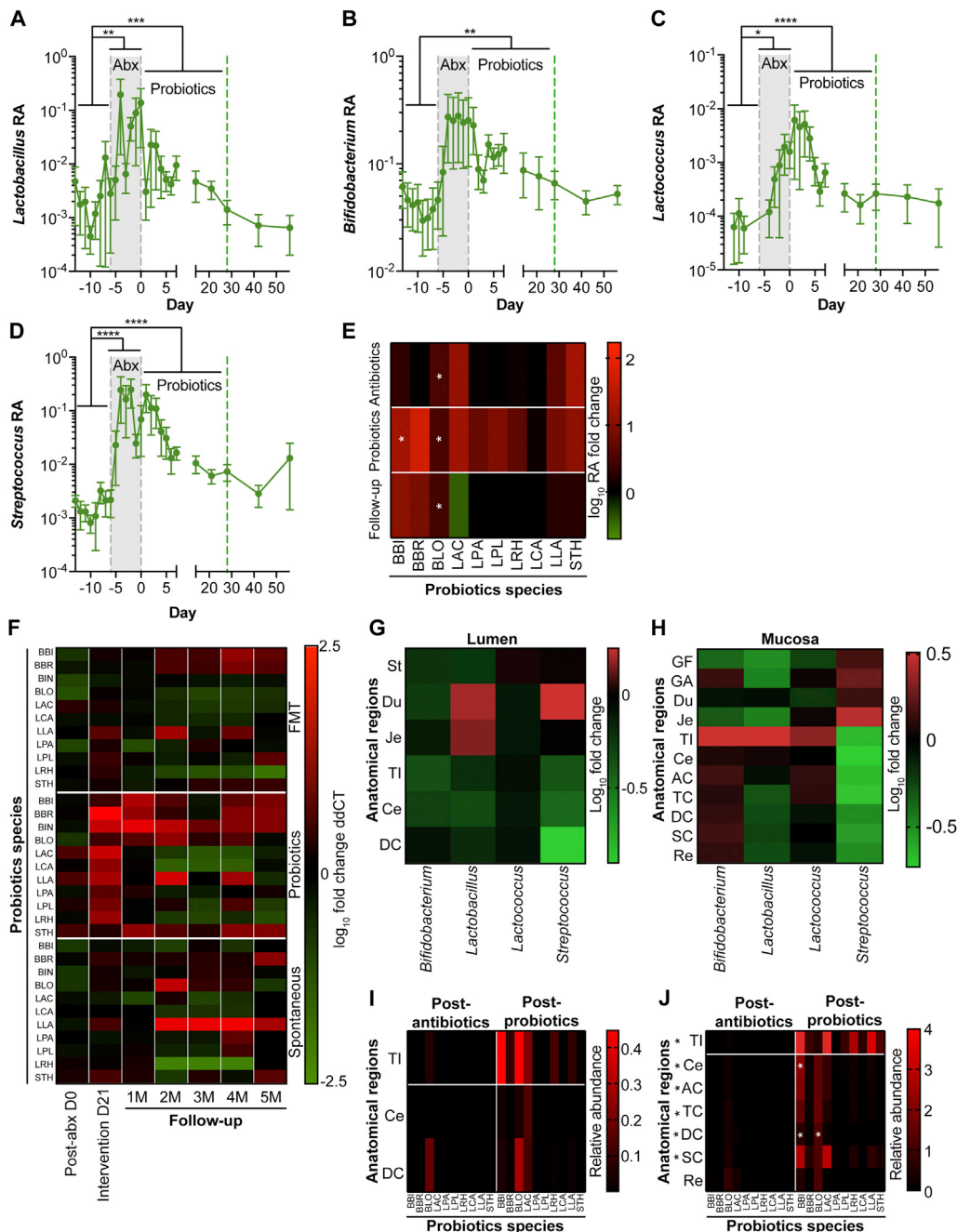


Figure S5. Spatial and Temporal Analysis of Probiotic Colonization in Antibiotic-Treated Humans, Related to Figure 3

(A-D) 16S rDNA-based quantification of probiotics-associated genera in stools of the probiotics consuming individuals, namely (A) *Lactobacillus* (B) *Bifidobacterium* (C) *Lactococcus* (D) *Streptococcus*. *p < 0.05; **p < 0.01; ***p < 0.001; ****p < 0.0001, Kruskal-Wallis & Dunn's.

(E) MetaPhlAn2-based quantification of probiotics species relative abundance in stools. *, any p < 0.05, Two-Way ANOVA & Dunnett compared to baseline.

(F) Probiotics species abundances as determined by qPCR in all participants from last day antibiotics till five months of follow up, normalized to baseline pre-antibiotics.

(G and H) 16S rDNA-based quantification of probiotics-associated genera in the (G) GI lumen or (H) mucosa of the probiotics-consuming individuals.

(I and J) Same as (F) and (G) but based on MetaPhlAn2. *, any p < 0.05, Two-Way ANOVA for tissues and Sidak per-species per-tissue. Symbols represent the mean; error bars SEM.

RA, relative abundance; Abx, antibiotics; Spont, spontaneous recovery; D, day; M, months.

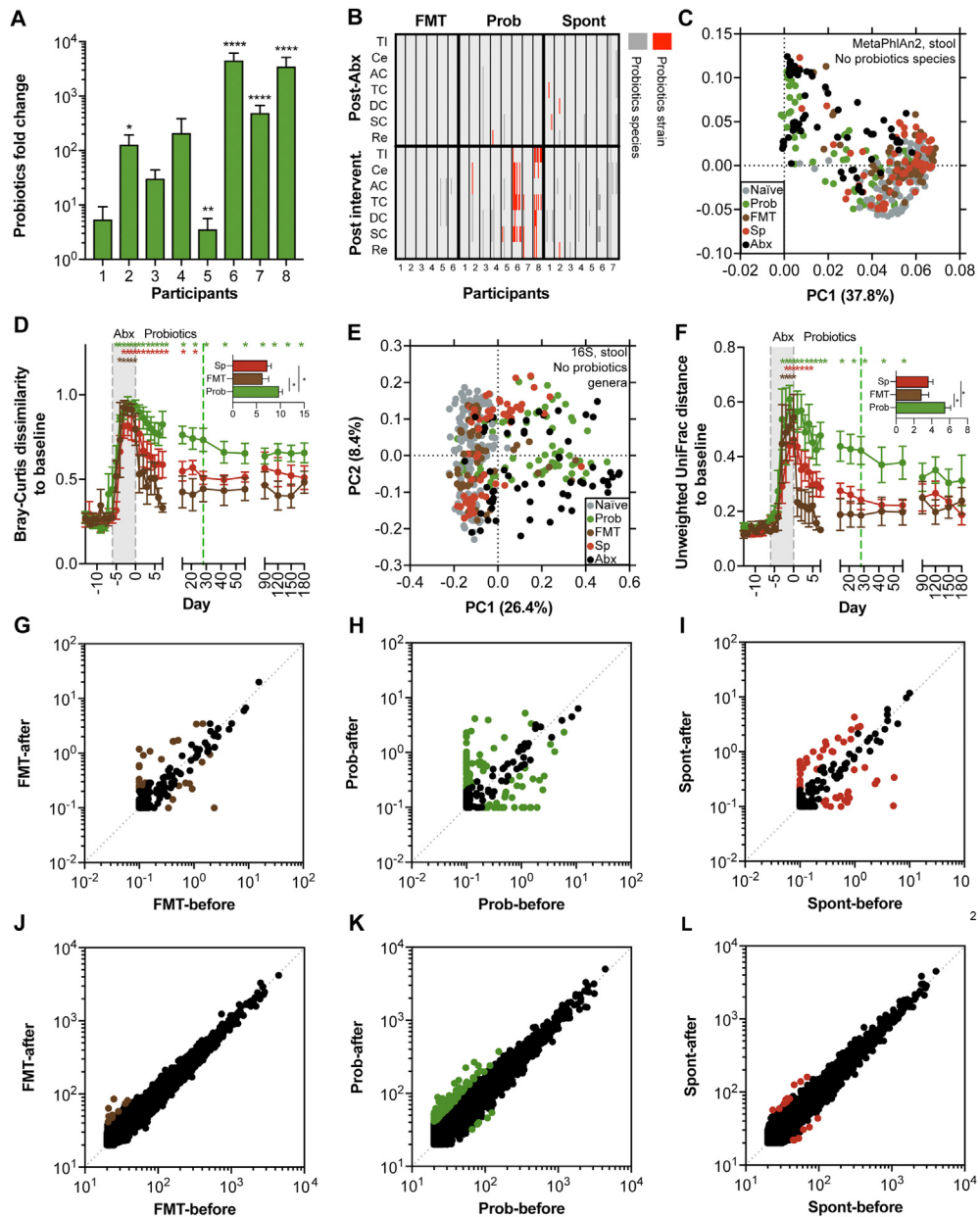


Figure S6. Probiotics Delay while aFMT Enhances Human Fecal Microbiome Reconstitution to Naivety following Antibiotics Treatment, Related to Figures 3 and 4

(A and B) Inter-individual differences in probiotics colonization in the antibiotics perturbed gut. (A) Average fold differences calculated between the last antibiotics and last probiotics supplementation day for each participant for each probiotics species in each region. * $p < 0.05$; ** $p < 0.01$; *** $p < 0.0001$, Wilcoxon signed-rank test. (B) Probiotics strain quantification in the GI mucosa based on mapping of metagenomic sequences to unique genes, which correspond to the strains found in the probiotics pill. Dark gray marks the presence of the probiotics species and red marks the presence of the probiotics strains.

(C and D) Species abundances were recalculated after omitting the 10 probiotics species from the MetaPhiAn2 output table and renormalizing to 1. (C) PCA plot of distances between stool samples collected during reconstitution in each of the treatment arms and during or before antibiotics (D) Bray-Curtis dissimilarity to baseline stool samples of each participant (mean of a group is plotted) throughout the experiment. Colored asterisks indicate significant difference of a time-point to baseline (any $p < 0.05$, Two-Way ANOVA & Dunnett). Inset, area under the post-abx reconstitution curve for each group. * $p < 0.05$, two-tailed t test.

(E and F) Same as (C and D) but for UniFrac distances recalculated after omitting the four probiotics genera (*Lactobacillus*, *Bifidobacterium*, *Lactococcus*, and *Streptococcus*) from the OTU table, followed by rarefaction to 10,000 reads and renormalizing to 1.

(G–I) Relative abundance of species before antibiotics and after (G) aFMT, (H) probiotics or (I) spontaneous recovery (spont).

(J–L) same as (G)–(I) but with KOs. Colored species or KOs remained more than 2-fold differential in their abundance before and after the treatment.

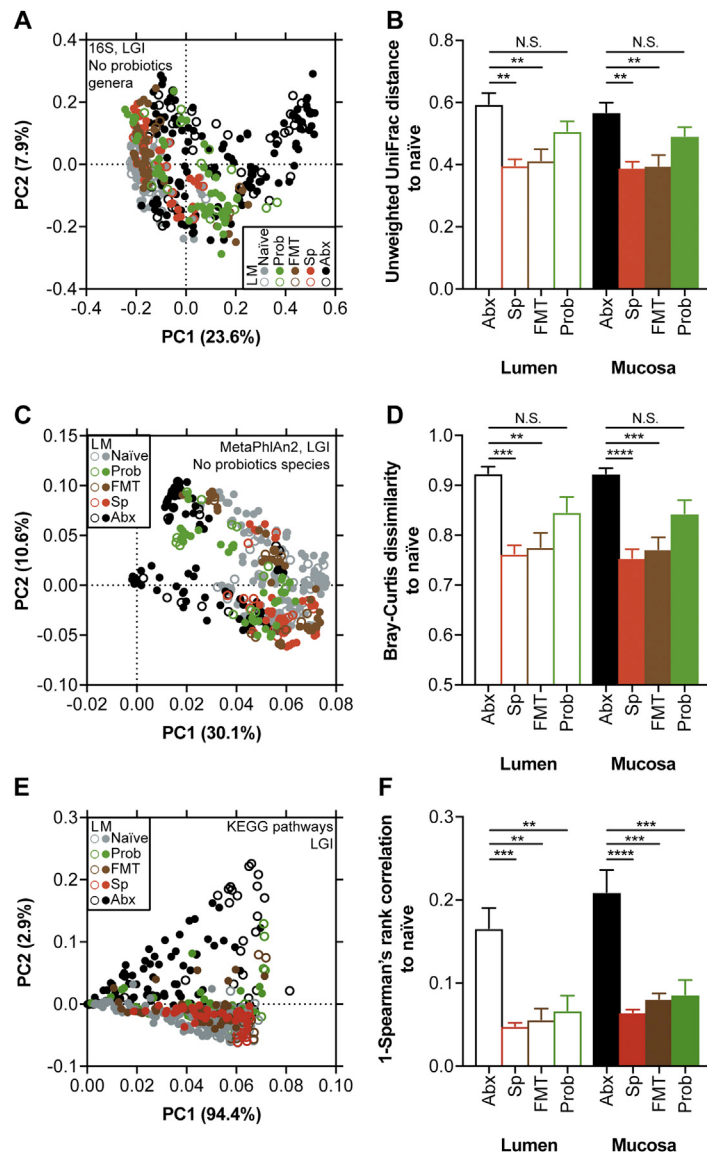


Figure S7. Probiotics Delay while aFMT Enhances Human Gut Microbial and Luminal Microbiome Reconstitution to Naivety following Antibiotics Treatment, Related to Figure 5

(A and B) UniFrac distances in LGI samples were recalculated after omitting the four probiotics genera (*Lactobacillus*, *Bifidobacterium*, *Lactococcus*, and *Streptococcus*) from the OTU table, followed by rarefaction to 10,000 reads and renormalizing to 1.

(C and D) Bray-Curtis dissimilarity indices were recalculated after omitting the 10 probiotics species from the MetaPhiAn2 output table and renormalizing to 1.

(E) PCA demonstrating reconstitution patterns three weeks after antibiotics treatment in each of the arms and antibiotics-naive individuals based on KEGG pathways.

(F) 1-Spearman correlation to the antibiotics-naive cohort based on KEGG pathways. **p < 0.01; ***p < 0.001; ****p < 0.0001, Mann-Whitney. Abx, antibiotics, Spontaneous recovery, Prob, probiotics.